NATIONAL ADVISORY COMMITTEE FOR AERONAUTICS

WARTIME REPORT

ORIGINALLY ISSUED

April 1944 as
Memorandum Report

TESTS OF NACA 65(216)-420 AND 66(218)-420

AIRFOILS AT HIGH SPEEDS

By Joseph L. Anderson

Ames Aeronautical Laboratory
Moffett Field, California

NACA

WASHINGTON

NATIONAL ADVISORY COMMITTEE FOR AERONAUTICS

MEMORANDUM REPORT

for the

Bureau of Aeronautics, Navy Department

TESTS OF NACA 65(216)-420 AND 66(218)-420

AIRFOILS AT HIGH SPEEDS

By Joseph L. Anderson

SUMMARY

Wind-tunnel tests of NACA 65(216)-420, a = 1.0, and 66(218)-420, a = 1.0, airfoils at speeds up to and slightly above the critical are described. The test Reynolds numbers extended from 4,000,000 to 17,000,000 for the 65-series airfoil and from 4,000,000 to 28,500,000 for the 66-series. Section coefficients of lift, drag, and pitching-moment and extensive pressure-distribution data are presented.

The critical speed for these airfoils at their design lift coefficient of 0.4 is shown to be about 460 miles per hour at sea level and about 415 miles per hour at 25,000 feet altitude. The 66(218)-420 airfoil was found to be extremely sensitive to surface imperfections. Throughout the test range the 65-series airfoil had no more and even less drag than the 66-series airfoil, and the low-drag characteristics extended over a greater range of lift coefficients.

INTRODUCTION

In order to provide data on the characteristics at high speeds, tests have been made of NACA 65(216)-420, a = 1.0, and 66(218)-420, a = 1.0, airfoils of 5-foot chord, and a 66(218)-420, a = 1.0, airfoil of 8-foot chord. The purpose of the latter was to determine the separate effects of Reynolds number and compressibility. The two profiles were chosen in order to determine the effects of rather high camber (0.4 ideal lift coefficient) and large thickness (20 percent of the chord) on the section characteristics of low-drag airfoils. All three were tested at speeds up to and slightly above the critical.

The test results for the NACA 66(218)-420 airfoil of 5-foot chord have recently been published (reference 1), but the coefficients were uncorrected for tunnel-wall effects. The corrected results are included in the present report.

APPARATUS AND METHOD

The tests were conducted in the Ames 16-foot high-speed wind tunnel, Moffett Field, Calif. This tunnel has a single return and a closed circular test section 16 feet in diameter.

In accordance with the NACA notation, the first number in the designating numbers of the airfoils, NACA 65(216)-420, $a = 1$, and 66(218)-420, $a = 1$, indicates that the sections are for low-drag airfoils of the 6 family. The second numbers, 5 and 6, indicate that the region of falling pressures extends from the leading edge to 50 and 60 percent of the chord, respectively. The numbers in the parentheses indicate the basic airfoil sections from which these airfoils were derived. The number 2 indicates that the low-drag range of the basic airfoil is for lift coefficients 0.2 more or less than the ideal. The numbers 16 and 18 indicate that the basic airfoil sections are 16 and 18 percent of the chord thick, respectively. The number 4, following the dash, indicates the ideal lift coefficient to be 0.4, the number 20 shows the thickness in percent of chord, and $a = 1$ is the designation of the camber line which gives a uniform chordwise lift distribution. The two airfoils are thus designed to have the same working range of lift coefficient, are cambered for the same ideal lift coefficient (0.4), have the same thickness (0.20 chord), and are designed for uniform chordwise distribution of lift.

The coordinates for the airfoil sections are given in figures 1 and 2. These coordinates were derived from those for symmetrical airfoils by the method explained in reference 2. All three airfoils were of constant chord. They completely spanned the test section of the wind tunnel, as shown in figure 3, except for clearance of one-eighth to three-sixteenths inch at the tunnel walls.

The airfoils were made of wood mounted on welded steel box spars. The airfoil sections stopped at the tunnel walls, but the spars extended through the walls to the trunnions of the balance frame, which supported the airfoils and provided

A-57

for adjustment of the angle of attack.

The airfoils were painted, sandpapered, and polished so that the surfaces were fair and true and, during the tests, they were maintained in this condition. The angles of attack were checked during the tests by means of torque tubes fastened to the airfoils at midspan and extended to reference fittings outside the test section of the tunnel. The torque tubes made it possible to determine the twist of the airfoils under load and to compensate for deformation so that the midspan section was kept at the desired angle of attack.

In each airfoil, 2.5 feet from the midspan, there was a chordwise row of 37 static pressure orifices. The orifices, 0.020 inch in diameter, were connected to a multiple-tube manometer which was photographed to obtain instantaneous and permanent records.

From measurements of the loss of momentum in the wake behind the airfoils, the drag coefficients of the airfoil section were computed. The momentum-loss measurements were made at the center of the span by means of a rake of total-pressure and static-pressure tubes connected to a multiple-tube manometer. The method of Silverstein and Katzoff (reference 3), as outlined by Davis in reference 4, was employed for computing the drag coefficients presented in this report.

The lift coefficients were derived by integrating plots of the pressure distribution to obtain the coefficients of normal force and applying the formula, given later, for lift coefficient in terms of normal force and drag for various angles of attack. Coefficients of pitching moment were computed by integrating the moments of the pressure as shown by plots parallel and normal to the chord.

For a few of the tests, in order to determine the effect of various surface conditions, the transition point was arbitrarily fixed at 10, 30, 50, or 60 percent of the chord aft of the leading edge on both the upper and lower surfaces by 1/2-inch-wide spanwise bands of No. 60 carborundum grains. The effect of "standard" roughness, as described in reference 5, was tested on only the NACA 65(216)-420 airfoil. Sheets of No. 60 carborundum paper extending around the leading edge of the airfoil for 10.5 inches constituted the "standard" roughness for this test.

COEFFICIENTS AND SYMBOLS

The coefficients used in this report are as follows:

c_n section normal-force coefficient $\left[1/c \int_c (S_U - S_L) dx \right]$

c_d section drag coefficient $\left(F/c \int_w \dfrac{H - H_l}{q} \, dy \right)$

c_l section lift coefficient $\left(\dfrac{c_n}{\cos \alpha} - c_d \tan \alpha \right)$

$c_{m_{c/4}}$ section pitching-moment coefficient
$$\left\{ 1/c^2 \left[\int_c (S_U - S_L)\left(\frac{c}{4} - x\right) dx + \int_c (S_U - S_L) y \, dy \right] \right\}.$$

S pressure coefficient $\left(\dfrac{H - p_l}{q} \right)$

P pressure coefficient $\left(\dfrac{p_l - p}{q} \right)$

R Reynolds number $\left(\dfrac{\rho V c}{\mu} \right)$

M Mach number $\left(\dfrac{V}{a} \right)$

where

c airfoil chord

S_U pressure coefficient, upper surface

S_L pressure coefficient, lower surface

x distance of pressure station from leading edge measured parallel to wing chord

F proportionality factor (reference 4)

w thickness of wing wake

$H = p + (1+\eta)q$ total pressure in free stream

H_l	total pressure in wing wake
q	free-stream dynamic pressure $(\frac{1}{2}\rho V^2)$
p	free-stream static pressure
$(1 + \eta)$	the compressibility factor (reference 6)

$$\left[(1 + \frac{M^2}{4} + \frac{M^4}{40} + \frac{M^6}{1600} - \frac{M^8}{80,000} + \ldots)\right]$$

y	ordinate of pressure station measured from wing chord
α	angle of attack of airfoil, degrees
p_l	local static pressure on airfoil surface
ρ	density of air in free stream
V	velocity of air in free stream
μ	viscosity of air in free stream
a	velocity of sound in free stream

The equation for the critical pressure coefficient of the form $(p_l - p)/q$, at which the speed of sound is reached locally, is

$$P_{cr} = \frac{1.43}{M^2}\left\{[0.834 (1 + 0.20 M^2)]^{3.5} - 1\right\}$$

(reference 7, page 6, equation (6A))

Since

$$S = \frac{H - p_l}{q} = \frac{p + q(1 + \eta) - p_l}{q} = (1 + \eta) - \left(\frac{p_l - p}{q}\right)$$

and

$$P = \frac{p_l - p}{q}$$

6

then

$$S = (1 + \eta) - P,$$

and, therefore the value of S at which sonic velocity is reached is

$$S_{cr} = (1 + \eta) - P_{cr}$$

Of use in this report is a theoretical equation for the rate of change of pressure coefficient with Mach number. An equation of von Kármán's (reference 8, page 347, equation (62)) is used. With von Kármán's symbol notation changed to that used in this report, the equation is

$$P_M = \frac{P_O}{\sqrt{1 - M^2} + \dfrac{M^2}{1 + \sqrt{1 - M^2}} \dfrac{P_O}{2}}$$

where

P_M pressure coefficient at a Mach number of M

P_O pressure coefficient at a Mach number of zero

von Kármán's equation in terms of S is then

$$S_M = (1 + \eta) - \frac{(1 - S_O)}{\sqrt{1 - M^2} + \dfrac{M^2}{1 + \sqrt{1 - M^2}} \left(\dfrac{1 - S_O}{2}\right)}$$

CORRECTIONS FOR TUNNEL-WALL EFFECTS

The results presented in this report have been corrected for tunnel-wall effects by a method developed at the Ames Aeronautical Laboratory. The following equations give the corrected section lift, drag, and moment coefficients, angle of attack, Mach number, and Reynolds number for these airfoils in terms of uncorrected values of these quantities, which are

indicated by the subscript u.

For the 5-foot-chord airfoils:

$$c_l = \left\{1 - \frac{1}{1 - M_u^2}\left[0.0282 + (2 - M_u^2)\,0.00846\right]\right\}c_{l_u}$$

$$c_d = \left\{1 - \left[\frac{2 - M_u^2}{1 - M_u^2} + \frac{1 + 0.4\,M_u^2}{\sqrt{1 - M_u^2}}\right]0.00846\right\}c_{d_u}$$

$$c_{m_{c/4}} = \left[1 - (0.00846)\left(\frac{2 - M_u^2}{1 - M_u^2}\right)\right]c_{m_{c/4u}} + \left(\frac{0.00705}{1 - M_u^2}\right)c_{l_u}$$

$$\alpha = \alpha_u + \frac{0.257}{\sqrt{1-M_u^2}}\left(c_{l_u} + 4\,c_{m_{c/4u}}\right)$$

$$M = \left[1 + \frac{0.00846}{1 - M_u^2}(1 + 0.2\,M_u^2)\right]M_u$$

$$R = (1.008)\,R_u$$

For the 8-foot-chord airfoil:

$$c_l = \left\{1 - \frac{1}{1 - M_u^2}\left[0.0722 + (2 - M_u^2)\,0.02165\right]\right\}c_{l_u}$$

$$c_d = \left[1 - \left(\frac{2 - M_u^2}{1 - M_u^2} + \frac{1 + 0.4\,M_u^2}{\sqrt{1 - M_u^2}}\right)0.02165\right]c_{d_u}$$

$$c_{m_{c/4}} = \left[1 - (0.02165)\left(\frac{2 - M_u^2}{1 - M_u^2}\right)\right]c_{m_{c/4u}} + \left(\frac{0.01805}{1 - M_u^2}\right)c_{l_u}$$

8

$$\alpha = \alpha_u + \frac{0.658}{\sqrt{1 - M_u{}^2}} \left(c_{l_u} + 4\, c_{m_{c/4\,u}} \right)$$

$$M = \left[1 + \frac{0.02165}{1 - M_u{}^2} (1 + 0.2\, M_u{}^2) \right] M_u$$

$$R = (1.022)\, R_u$$

The pressure coefficients presented herein were corrected for tunnel-wall effects by the application of analogous equations.

RESULTS AND DISCUSSION

The data presented fall naturally into five sections. The first three sections include the lift, drag, and pitching-moment characteristics, as well as the critical Mach numbers of the individual airfoils. These results appear in the following order: NACA 66(218)-420, 5-foot chord (figs. 4 to 10); NACA 66(218)-420, 3-foot chord (figs. 11 to 17); and NACA 65(216)-420, 5-foot chord (figs. 18 to 25). In the fourth section, comparisons of the section characteristics of the three airfoils for various conditions are shown (figs. 26 to 35). The last section contains pressure-distribution data for the three airfoils at several angles of attack and for Mach numbers including the critical Mach number (figs. 36 to 51).

Of the NACA 65(216)-420 and 66(218)-420 airfoils of 5-foot chord, at $0°$ angle of attack and with the surface smooth, the NACA 65(216)-420 had an equal or lower drag coefficient throughout the range of Mach numbers of the tests. Figure 26 shows that at a Mach number of 0.15 the two airfoils had the same drag coefficient 0.0041 and at a Mach number of 0.55 the 65(216)-420 airfoil had a drag coefficient of only 0.0043; whereas that for the 66(218)-420 airfoil was 0.0049. The rapid drag increases shown in figure 27 at Reynolds numbers of approximately 17,000,000 and 28,000,000 for the 5-foot-chord and 3-foot-chord airfoils, respectively, are due primarily to compressibility shock rather than scale effect.

Figure 33 shows that the minimum drag coefficient of the NACA 65(216)-420 airfoil was 0.0002 less than for the

A-87

66(218)-420 airfoil. Also, the 65-series airfoil maintained its low-drag characteristics over a range of lift coefficients greater by 0.2 than the 66-series airfoil. The results in figure 33 are for a Mach number of 0.4; comparison of figure 7 with figure 21 shows that the 65-series airfoil had the lower drag coefficient for most of the angles of attack and Mach numbers included in the tests.

Figure 30 shows that the NACA 66(218)-420 has a slightly higher critical Mach number (0.015) at the design lift coefficient of 0.4 than the NACA 65(216)-420, 5-foot-chord airfoil. The small difference, less than 1 percent, between the critical Mach numbers of the NACA 66(218)-420, 5-foot- and 8-foot-chord airfoils is well within the limit of experimental accuracy. The critical Mach number is about 0.60 at the design lift coefficient and corresponds to 460 miles per hour at sea level or 415 miles per hour at 25,000 feet altitude.

In figures 6, 13, and 20 von Kármán's theoretical relation (reference 8) for the rate of increase of pressure coefficient with increase of Mach number is shown. The results for these three airfoils indicate that von Kármán's theory predicts the critical speed of the airfoils to be higher than it actually is.

For Mach numbers below the critical, fixing the transition point resulted in an almost constant increase of drag coefficient for each airfoil and roughness condition (figs. 4, 5, 11, 12, 18, and 19), except for the roughness at 60 percent of the chord on the NACA 66(218)-420, 8-foot-chord airfoil. With this airfoil the increase of drag coefficient with speed indicated that the transition point was probably moving forward (fig. 12(a)). The data also show that for Reynolds numbers from 23,000,000 to 28,000,000 the drag coefficient for this condition was greater than with roughness at 30 percent of the chord. The roughness at 60 percent of the chord may have contributed to separation over the rear portion of the airfoil after the transition point moved forward, which might have been the cause for the larger drag coefficient.

Comparison of figures 4 and 18 shows the NACA 65(216)-420 5-foot-chord airfoil to be less affected by roughness than the NACA 66(218)-420. This characteristic was brought out very markedly during the tests. Minute imperfections in the

10

surface of the 66-series airfoil caused an appreciable increase of drag coefficient (about 0.0005), while the 65-series airfoil was much less sensitive to surface imperfections.

Figure 27 shows that of the NACA 66(218)-420, 5-foot-and 8-foot-chord airfoils, the 5-foot-chord airfoil had a lower drag coefficient than the 8-foot for Reynolds numbers of 12,000,000 to 17,000,000. A Reynolds number of 15,000,000 corresponds to a Mach number of 0.465 for the 5-foot-chord airfoil and to 0.27 for the 8-foot airfoil. Figures 36 and 37 show that at these Mach numbers the 5-foot-chord airfoil has a more favorable pressure gradient than the 8-foot airfoil and therefore is more favorable to laminar flow over the forward wing surface. This steeper pressure gradient on the 5-foot-chord airfoil might have caused more extensive laminar flow, thus reducing the drag coefficient in comparison to that for the 8-foot-chord airfoil.

The NACA 65(216)-420, 5-foot-chord airfoil at angles of attack of 2.1°, 3.1°, and 4.2°, and for Mach numbers just below the critical value (fig. 21) is another example of beneficial compressibility effects on the drag coefficient. For these angles of attack, the pressure distribution over the upper surface of this airfoil (figs. 48 and 49) was rather flat for Mach numbers up to about 0.4. With the small pressure gradient, the transition point probably moved forward with increasing speed but, at Mach numbers above about 0.4, compressibility made the gradient more favorable to laminar flow.

Because of the large size of the airfoils relative to the wind tunnel, the maximum normal-force coefficients shown in figures 10, 17, 24, 25, 34, and 35 probably do not accurately represent free-air conditions.

CONCLUSIONS

The results of tests presented in this report lead to the following conclusions:

1. For most of the angles of attack and Mach numbers of these tests, the NACA 65(216)-420, 5-foot-chord airfoil has a lower drag coefficient than the NACA 66(218)-420 5-foot-chord airfoil, and the low-drag characteristics of the 65-series airfoil extend over a greater lift-coefficient range than for the

A-67

66-series airfoil.

    2. The NACA 66(218)-420 airfoil is more sensitive to minute surface imperfections than the NACA 65(216)-420 airfoil.

    3. The NACA 66(218)-420 airfoil has a slightly higher critical Mach number (greater by 0.015) than the NACA 65(216)-420 airfoil.

    4. For these airfoils, von Kármán's relation for the rate of increase of pressure coefficients with Mach number leads to overestimation of the critical speed.

Ames Aeronautical Laboratory,
    National Advisory Committee for Aeronautics,
        Moffett Field, Calif.

REFERENCES

1. Hood, Manley J., and Anderson, Joseph L.: Tests of an NACA 66,2-420 Airfoil of 5-Foot Chord at High Speed. NACA ACR, Sept. 1942.

2. Jacobs, Eastman N., Abbott, Ira H., and Davidson, Milton: Preliminary Low-Drag-Airfoil and Flap Data from Tests at Large Reynolds Numbers and Low Turbulence. NACA ACR, Mar. 1942, and Supplement.

3. Silverstein, A., and Katzoff, S.: A Simplified Method for Determining Wing Profile Drag in Flight. Jour. of the Aero. Sci., vol. 7, no. 7, May 1940.

4. Davis, Wallace F.: Comparison of Various Methods for Computing Drag from Wake Surveys. NACA ARR, Jan. 1943.

5. Jacobs, Eastman N., Abbott, Ira H., and Davidson, Milton: Investigation of Extreme Leading-Edge Roughness on Thick Low-Drag Airfoils to Indicate Those Critical to separation. NACA CB, June 1942.

6. Stack, John: The NACA High-Speed Wind Tunnel and Tests of Six Propeller Sections. Rep. No. 463, NACA 1933.

12

7. Robinson, Russell G., and Wright, Ray H.: Estimation of
    Critical Speeds of Airfoils and Streamline Bodies. NACA
    ACR, Mar. 1940.

8. von Kármán, Th.: Compressibility Effects in Aerodynamics.
    Jour. of the Aero. Sci., vol 8, no. 9, July 1941.

A-87
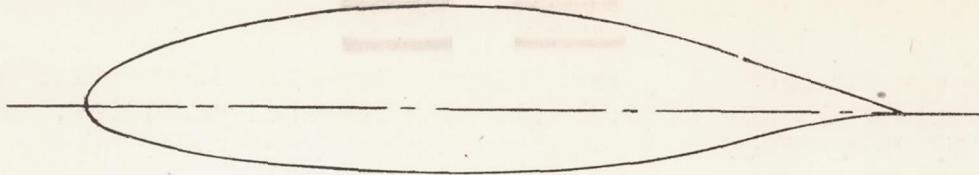
UPPER SURFACE		LOWER SURFACE	
STATION	ORDINATE	STATION	ORDINATE
0	0	0	0
0.235	1.676	0.765	-1.476
0.455	2.039	1.045	-1.759
0.916	2.613	1.584	-2.185
2.122	3.614	2.878	-2.870
4.587	5.039	5.413	-3.775
7.074	6.169	7.926	-4.473
9.575	7.115	10.425	-5.047
14.599	8.603	15.401	-5.911
19.640	9.742	20.360	-6.558
24.691	10.626	25.390	-7.046
29.748	11.295	30.252	-7.407
34.809	11.770	35.191	-7.650
39.872	12.067	40.128	-7.783
44.936	12.188	45.064	-7.808
50.000	12.135	50.000	-7.723
55.062	11.871	54.938	-7.491
60.119	11.381	59.881	-7.097
65.167	10.535	64.833	-6.415
70.200	9.338	69.800	-5.450
75.215	7.923	74.785	-4.340
80.211	6.367	79.789	-3.183
85.186	4.704	84.814	-2.012
90.139	3.017	89.861	-0.949
95.069	1.375	94.931	-0.111
100.000	0	100.000	0

L.E. RAD. 2.83

FIGURE 1.— COORDINATES OF THE NACA 66(218)~920, a=1, AIRFOIL IN PERCENT OF CHORD.
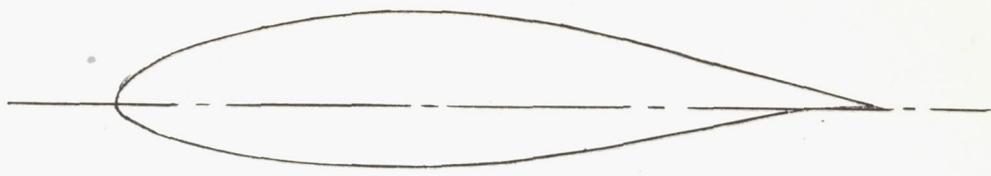
Upper Surface		Lower Surface	
Station	Ordinate	Station	Ordinate
0	0	0	0
0.250	1.582	0.750	-1.382
0.477	1.898	1.023	-1.618
0.941	2.438	1.559	-2.010
2.137	3.485	2.863	-2.741
4.587	5.042	5.413	-3.778
7.070	6.226	7.930	-4.530
9.568	7.212	10.432	-5.144
14.589	8.783	15.411	-6.091
19.631	9.960	20.369	-6.776
24.683	10.850	25.317	-7.270
29.742	11.497	30.258	-7.609
34.806	11.923	35.194	-7.803
39.871	12.135	40.129	-7.851
44.937	12.113	45.063	-7.733
50.000	11.796	50.000	-7.384
55.057	11.170	54.943	-6.790
60.105	10.260	59.895	-5.976
65.139	9.118	64.861	-4.998
70.159	7.833	69.841	-3.945
75.163	6.460	74.837	-2.880
80.152	5.038	79.848	-1.854
85.125	3.614	84.875	-0.922
90.086	2.259	89.914	-0.191
95.040	1.055	94.960	+0.209
100.000	0	100.000	0

L.E. RAD. 2.47

FIGURE 2. — COORDINATES OF THE NACA 65(216)-420, a=1,
AIRFOIL IN PERCENT OF CHORD
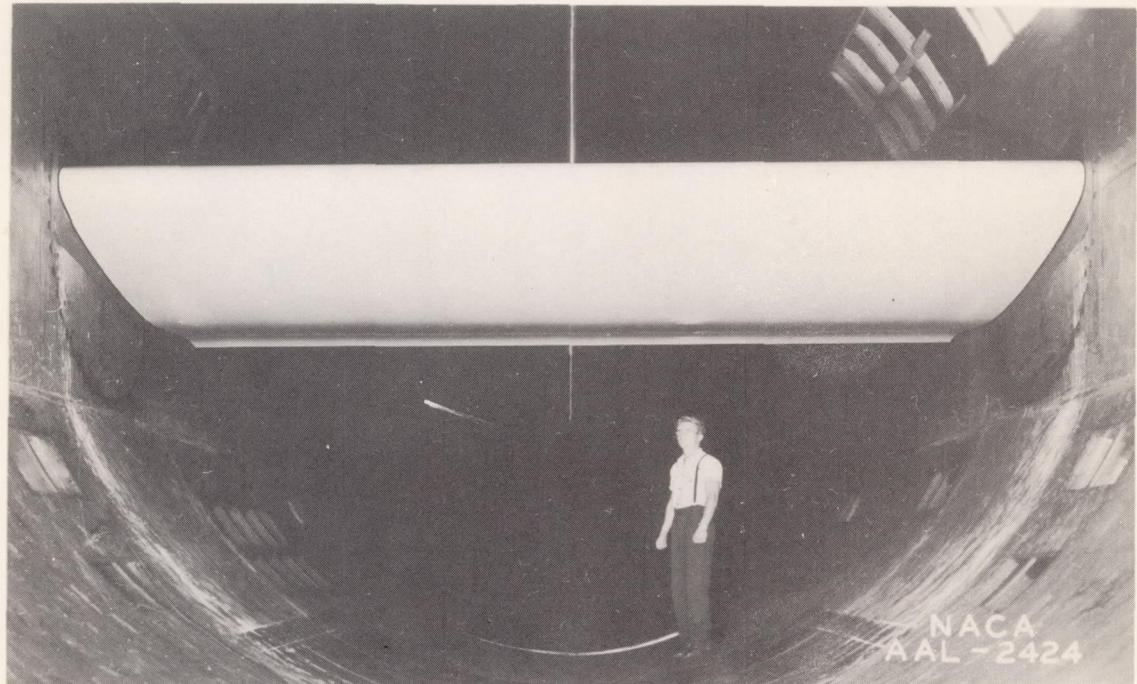
Figure 3.-An NACA 66(218)-420, 8-foot-chord airfoil
in the wind tunnel with the momentum rake in place.
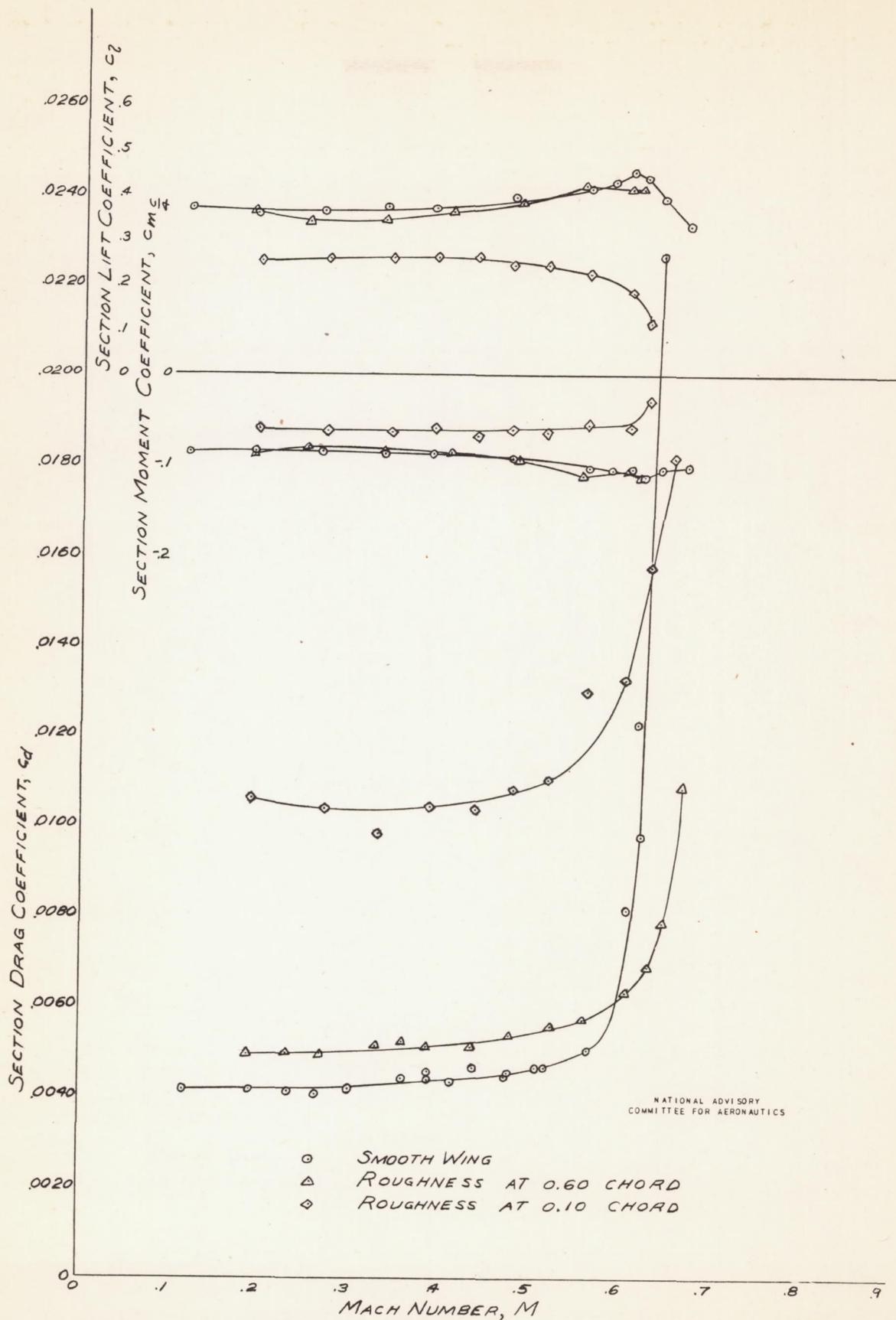
FIGURE 4. - VARIATION OF THE SECTION COEFFICIENTS WITH MACH
NUMBER FOR VARIOUS SURFACE CONDITIONS. ∝ = 0°,
NACA 66(218)-420 AIRFOIL, 5-FOOT CHORD.
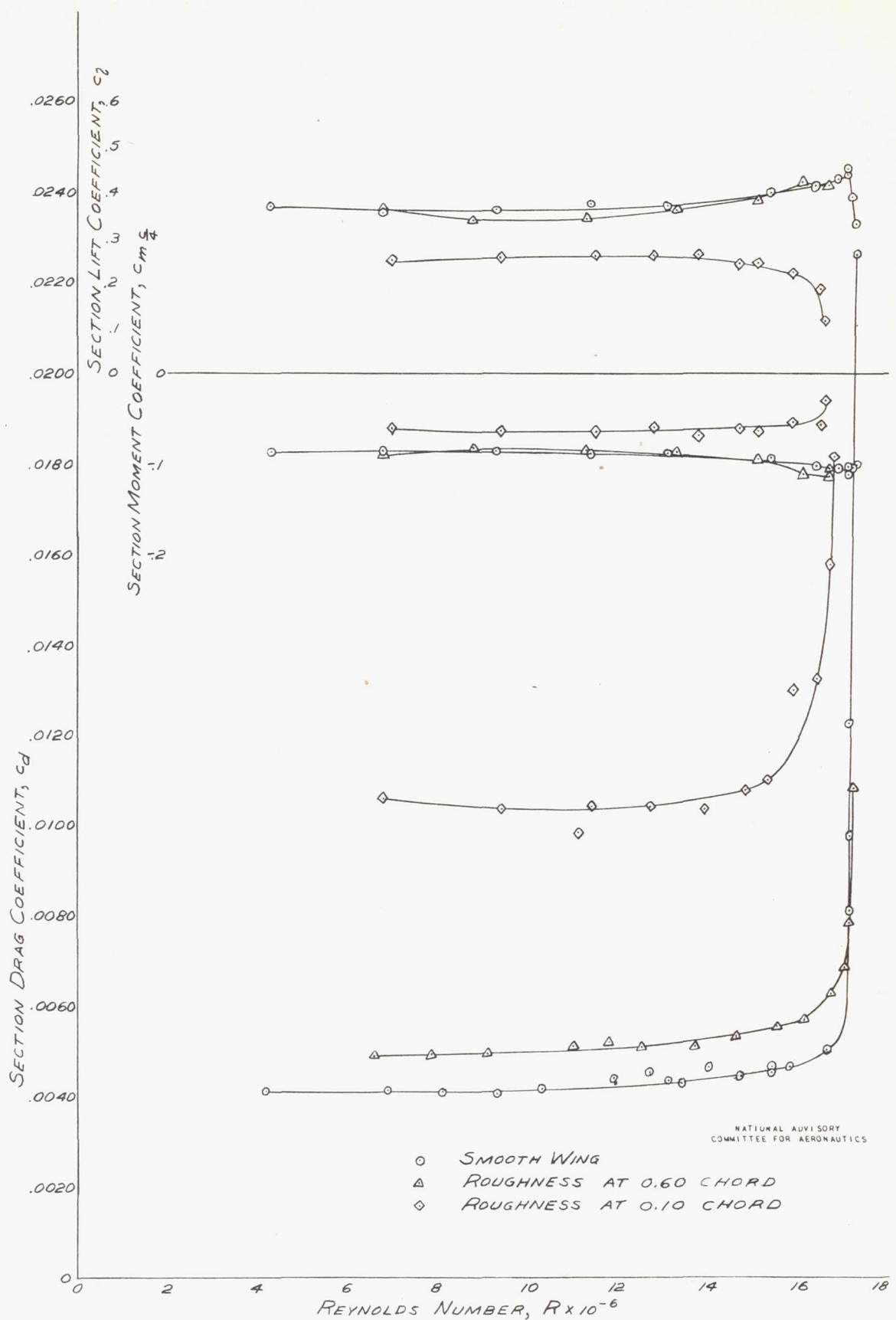
FIGURE 5. — VARIATION OF THE SECTION COEFFICIENTS WITH REYNOLDS NUMBER FOR VARIOUS SURFACE CONDITIONS. $\alpha = 0°$, NACA 66(218)-420 AIRFOIL, 5-FOOT CHORD.
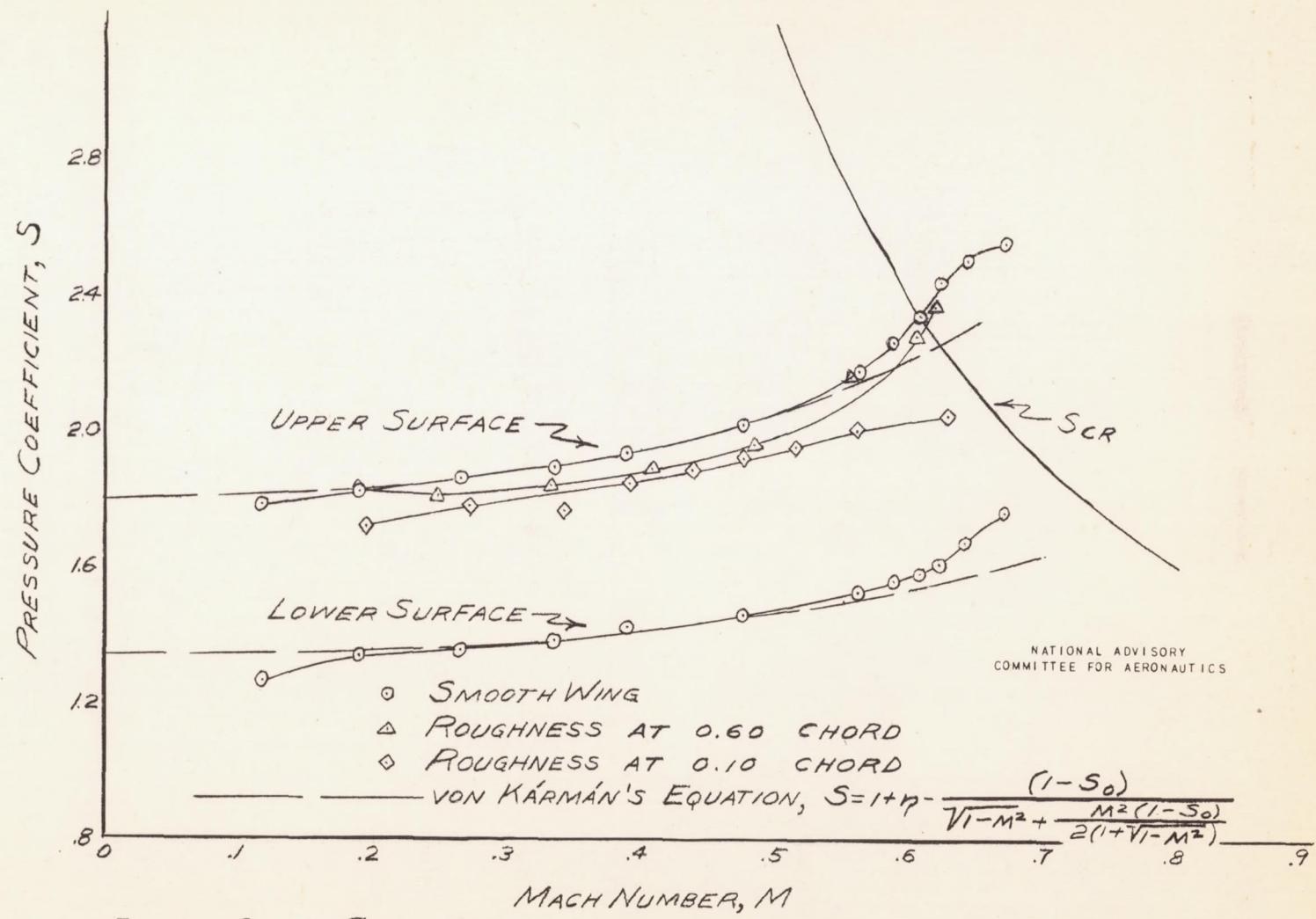
FIGURE 6. — EFFECT OF COMPRESSIBILITY AND SURFACE CONDITION ON THE MINIMUM PRESSURE COEFFICIENTS. $\alpha = 0°$, NACA 66(218)-420 AIRFOIL, 5-FOOT CHORD.
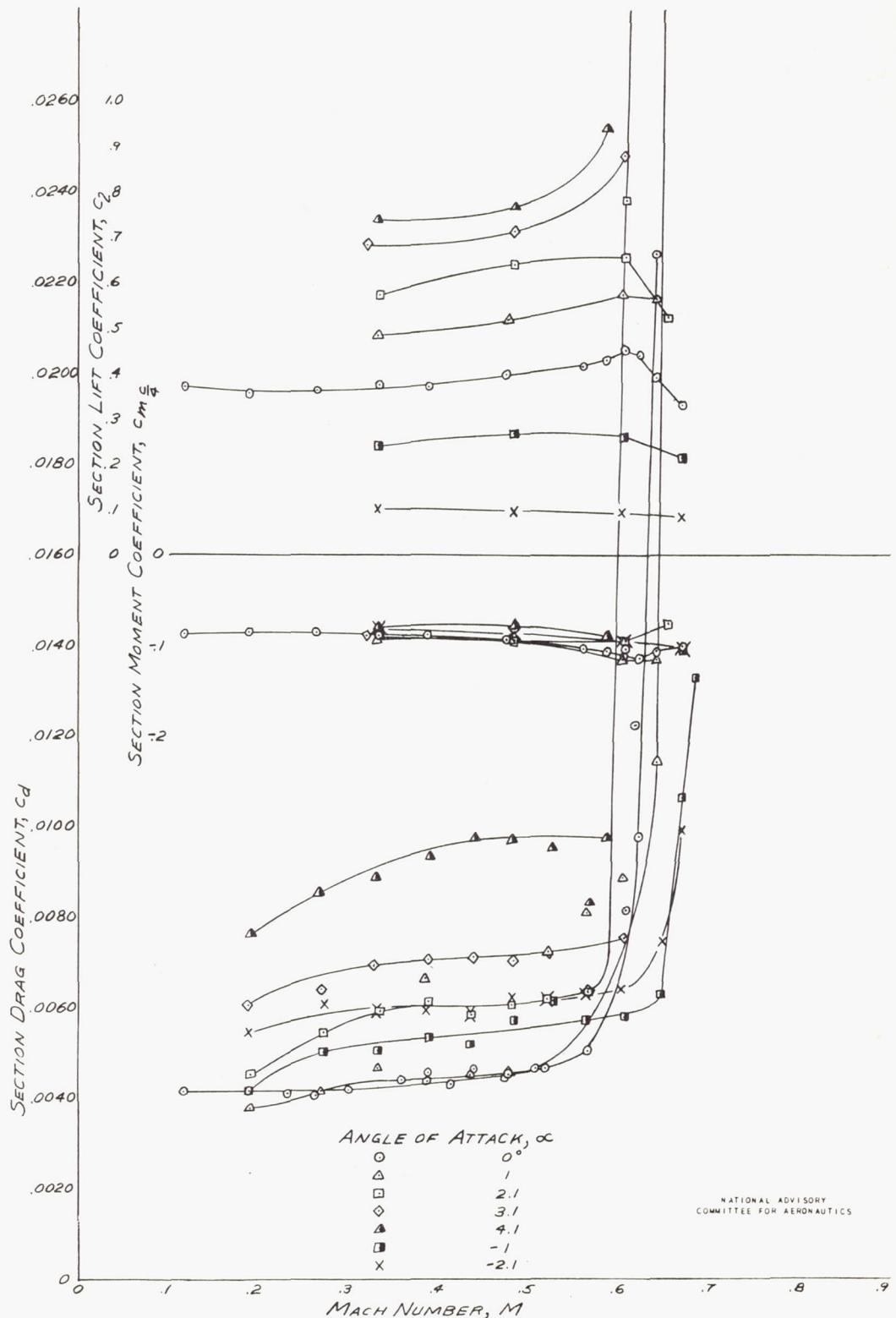
FIGURE 7. — VARIATION OF THE SECTION COEFFICIENTS WITH MACH
NUMBER AND ANGLE OF ATTACK.
NACA 66(218)-420 AIRFOIL, 5-FOOT CHORD.
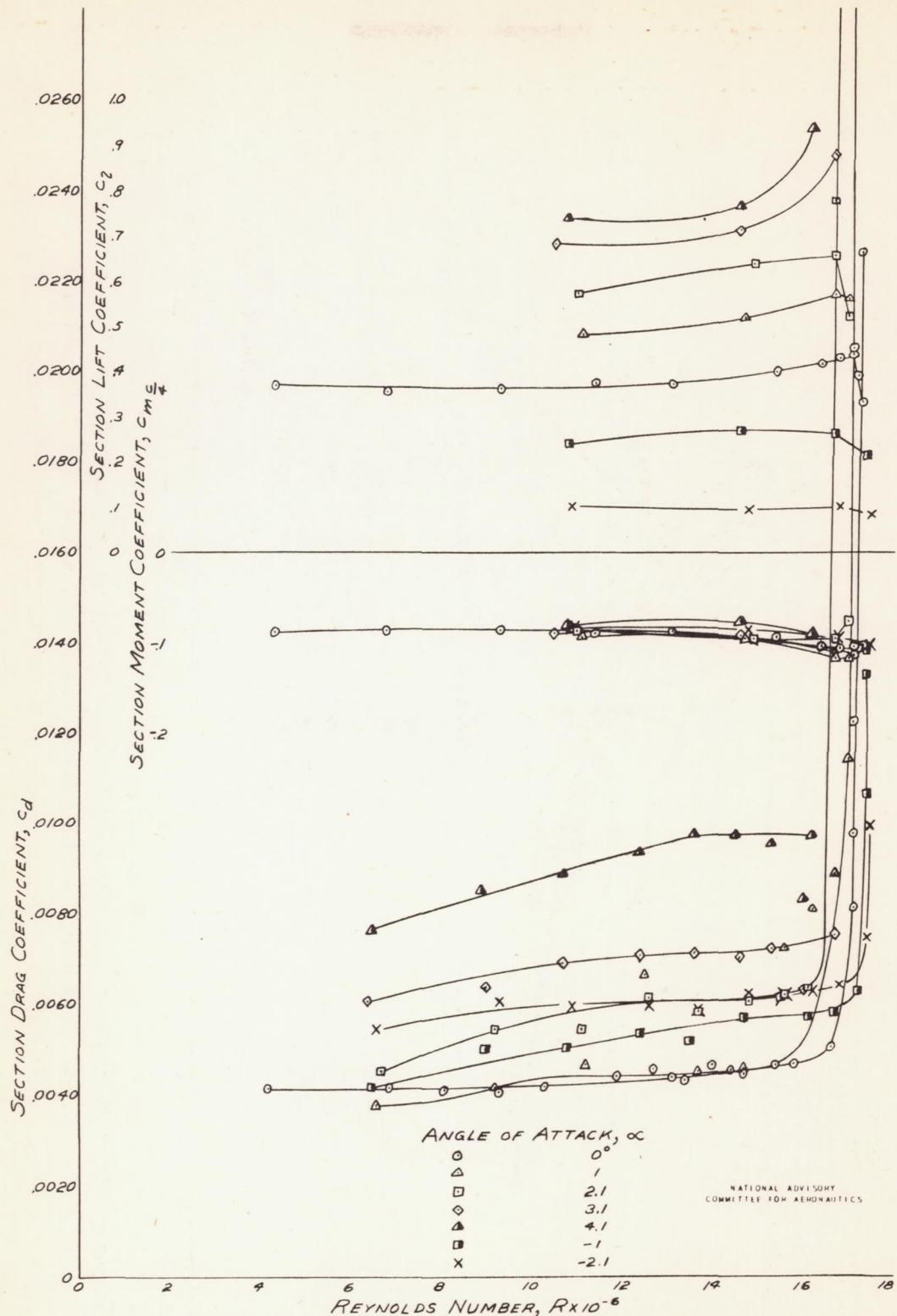
FIGURE 8. — VARIATION OF THE SECTION COEFFICIENTS WITH REYNOLDS
NUMBER AND ANGLE OF ATTACK.
NACA 66(218)-420 AIRFOIL, 5-FOOT CHORD.
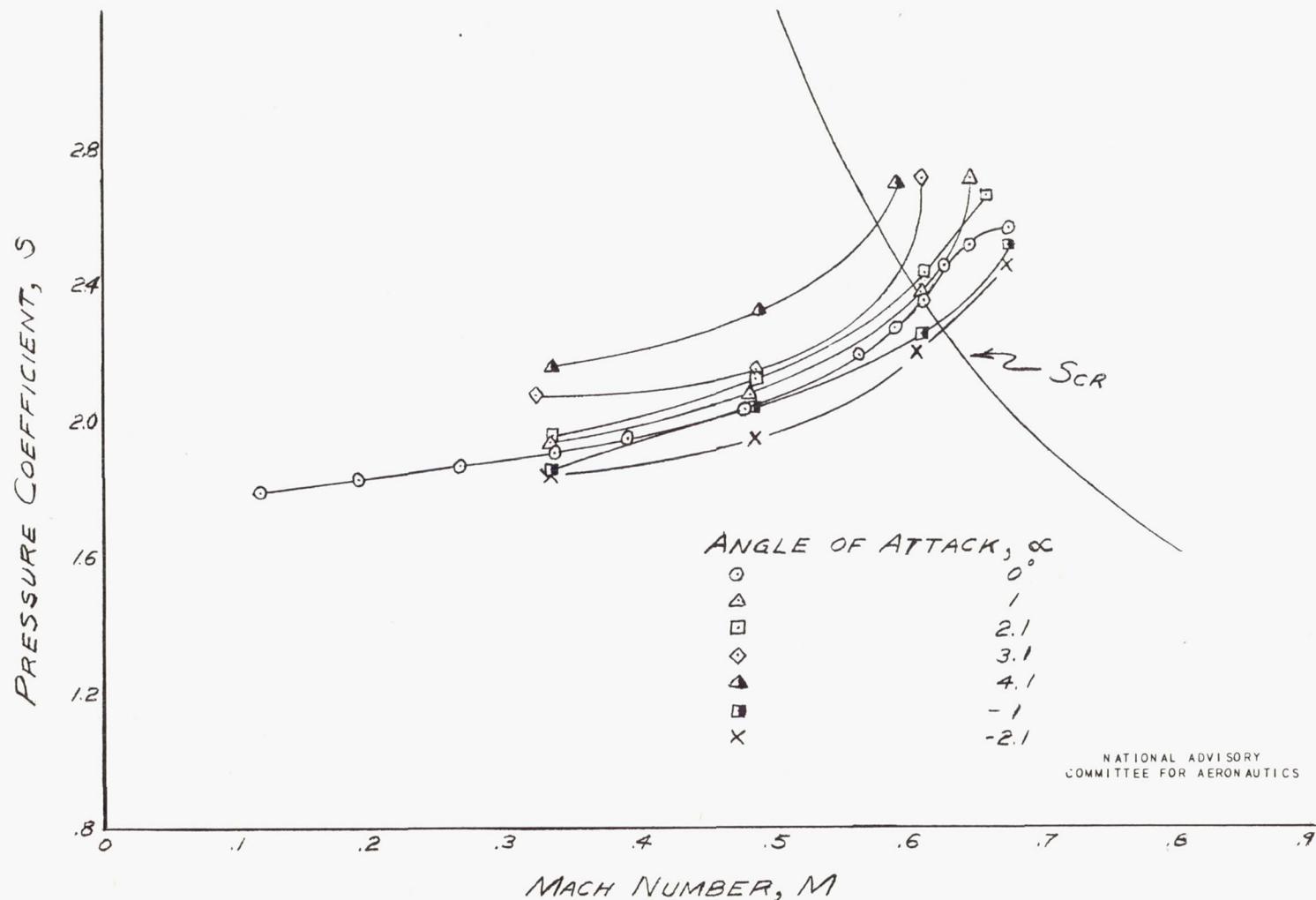
FIGURE 9. — EFFECT OF COMPRESSIBILITY AND ANGLE OF ATTACK ON
THE MINIMUM PRESSURE COEFFICIENT OF THE UPPER
SURFACE. NACA 66(218)-420 AIRFOIL, 5-FOOT CHORD.

SECTION NORMAL FORCE COEFFICIENT, c_n

1.6

1.2

.8

.4

○ SMOOTH WING
 M=0.189, R= 6.7×10

△ ROUGHNESS AT 0.10
 M=0.188 R= 6.6×10`

-24   -16   -8   0   8   16   24

ANGLE OF ATTACK, α

$C_{m\frac{c}{4}}$

-.4 -.04

SECTION MOMENT COEFF., $c_{m\frac{c}{4}}$

-1.2 -.12

-1.6 -.16
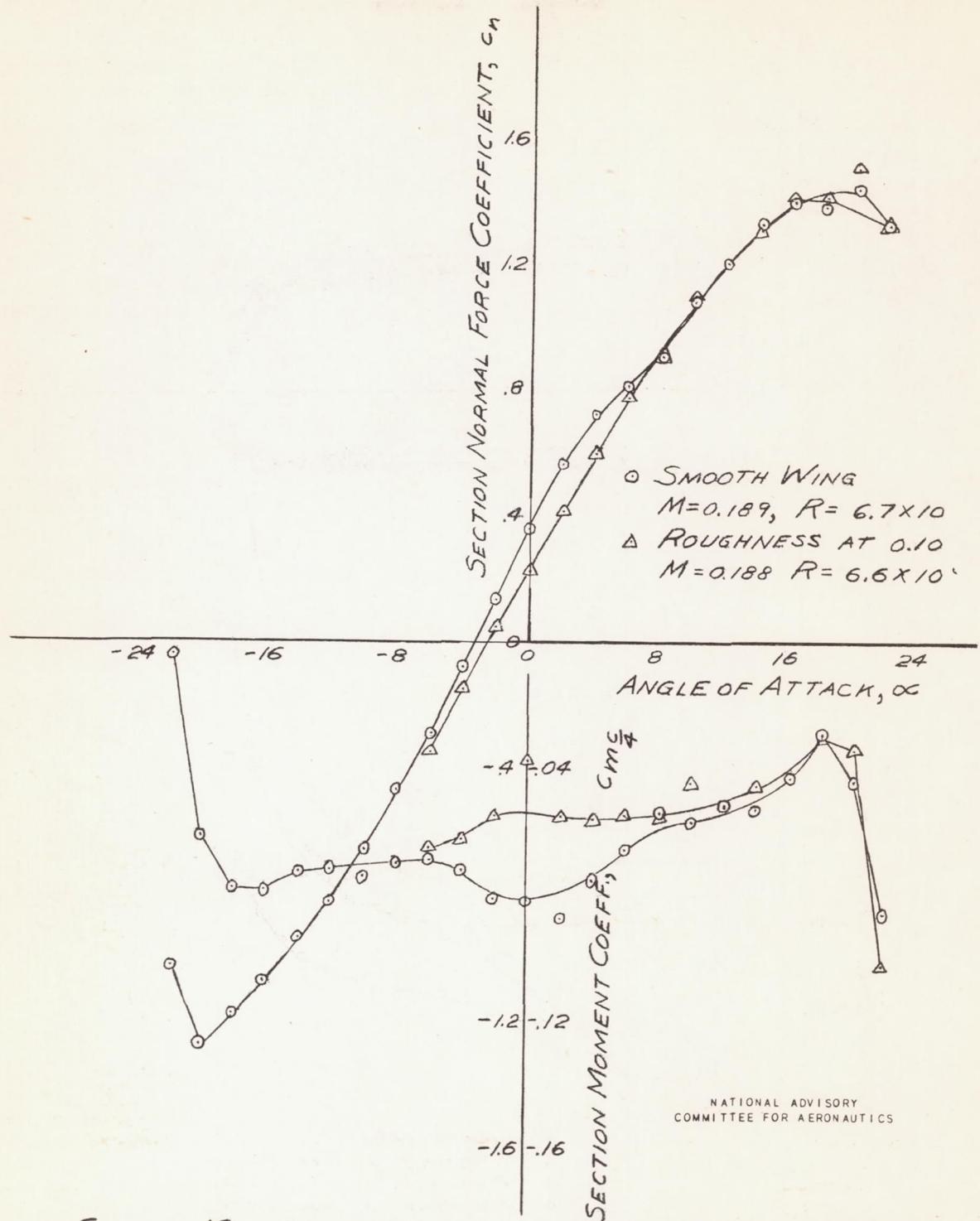
FIGURE 10. - VARIATION OF SECTION COEFFICIENTS WITH
ANGLE OF ATTACK THROUGH STALL CONDITION.
NACA 66(218)-420 AIRFOIL, 5-FOOT CHORD.
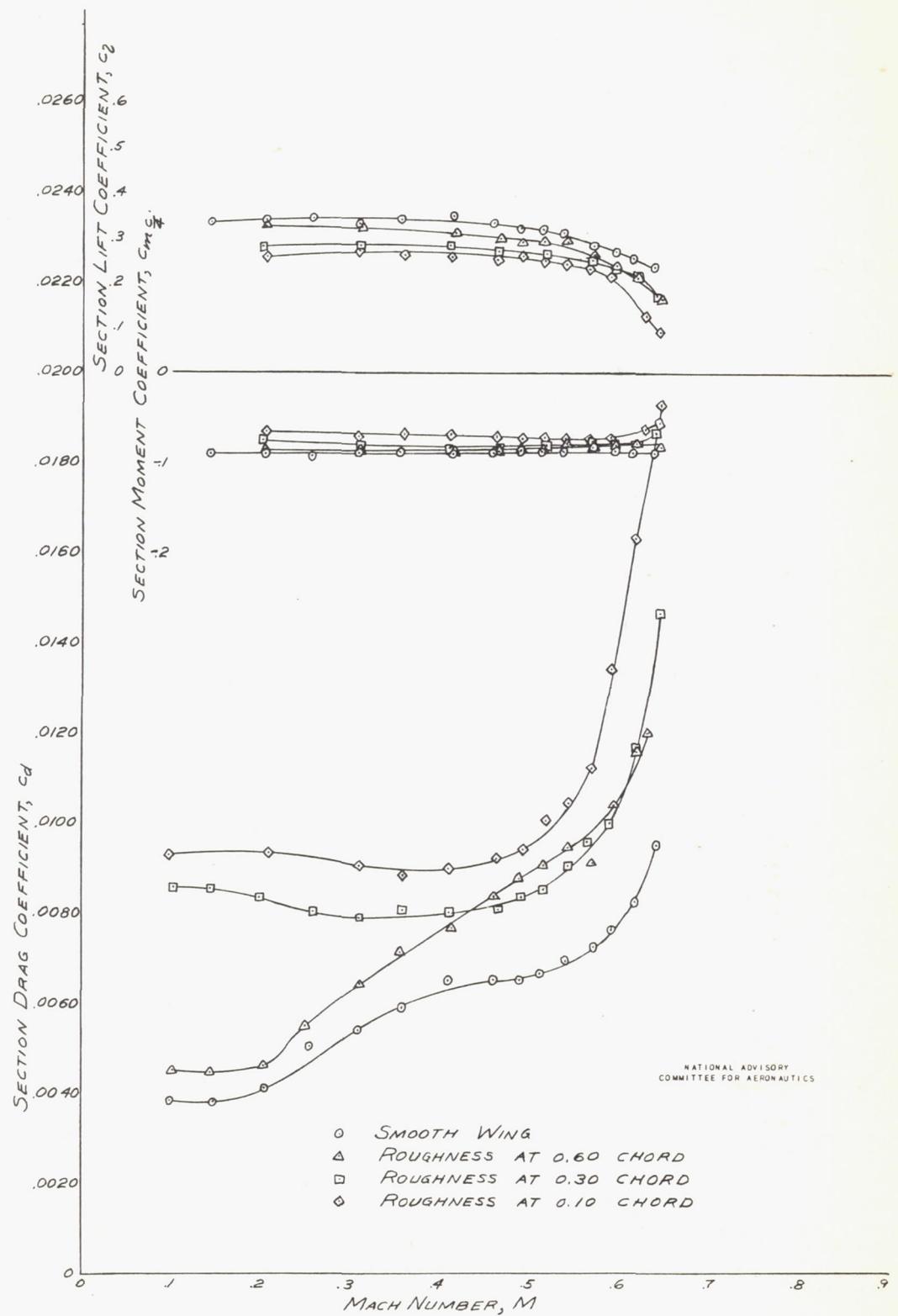
FIGURE 11. - VARIATION OF THE SECTION COEFFICIENTS WITH MACH NUMBER FOR VARIOUS SURFACE CONDITIONS. $\alpha = 0°$, NACA 66(218)-420 AIRFOIL, 8-FOOT CHORD.
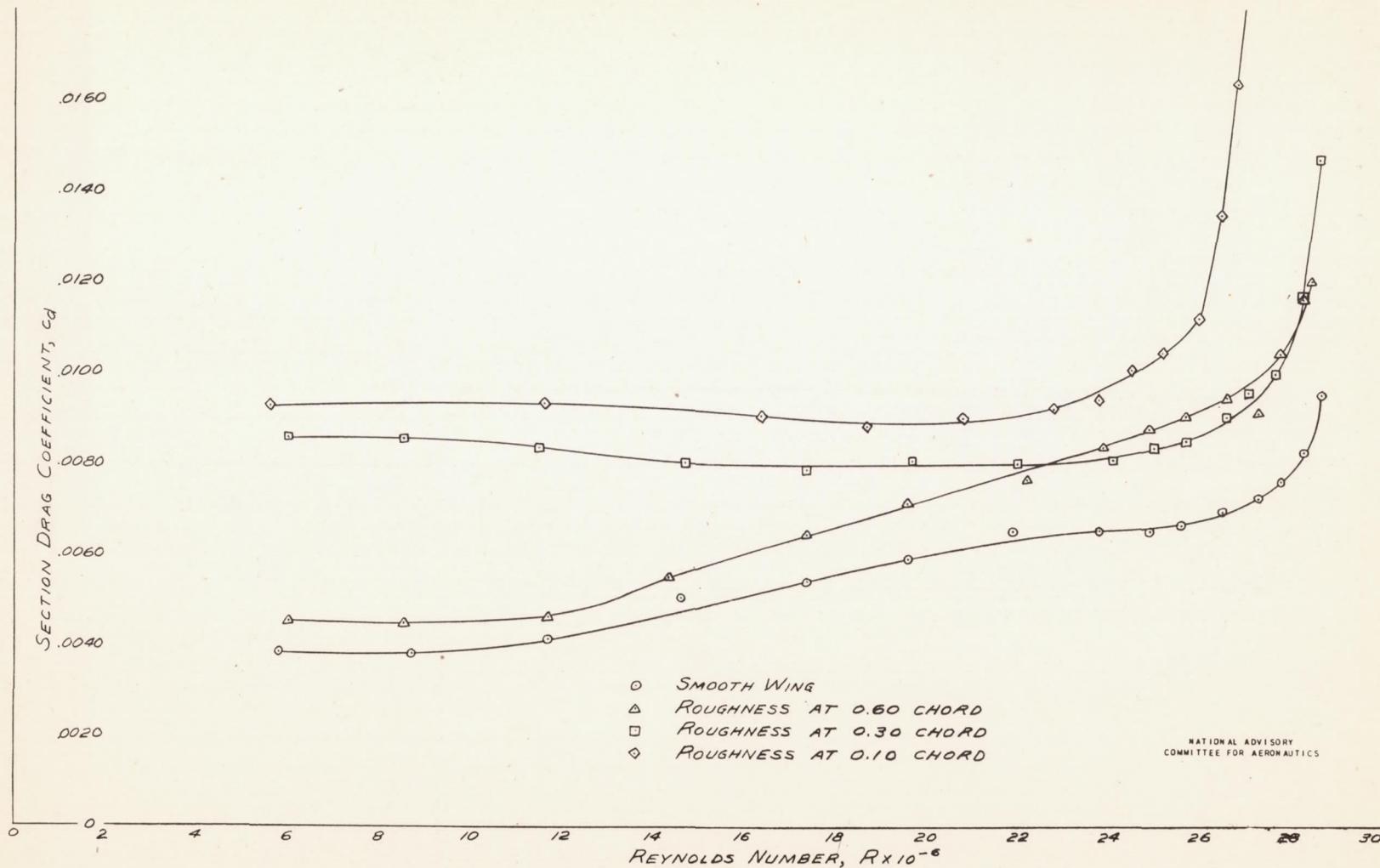
FIGURE 12(a).-VARIATION OF THE SECTION DRAG COEFFICIENT WITH REYNOLDS NUMBER FOR VARIOUS SURFACE CONDITIONS. $\alpha = 0°$; NACA 66(218)-420 AIRFOIL, 8 FOOT CHORD.

Section Lift Coefficient, c_l

Section Moment Coefficient, $c_m \frac{c}{4}$

.6
.5
.4
.3
.2
.1
0

Reynolds Number, $R \times 10^{-6}$

2   4   6   8   10   12   14   16   18   20   22   24   26   28   30

-.1
-.2

○   Smooth Wing
△   Roughness at 0.60 Chord
□   Roughness at 0.30 Chord
◇   Roughness at 0.10 Chord
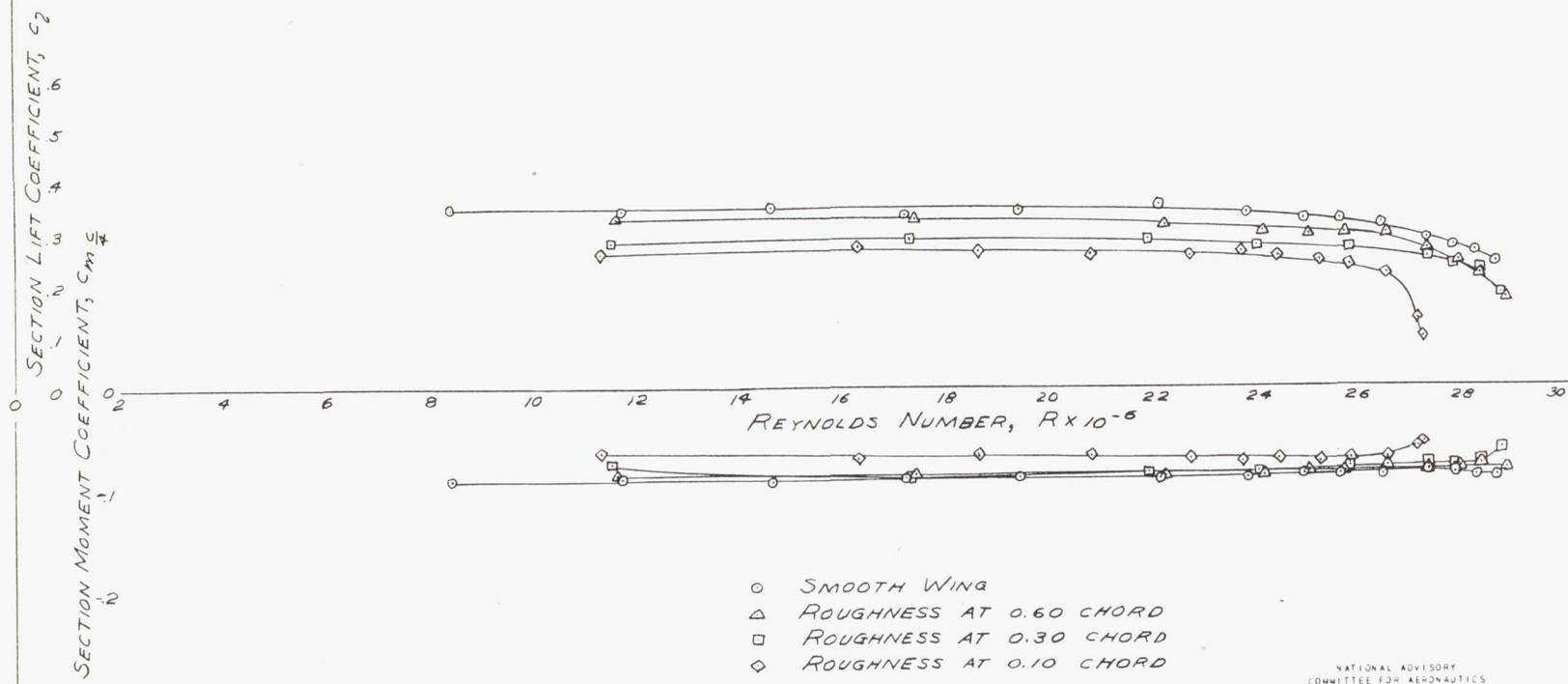
Figure 12(b). - Variation of the section lift and pitching moment coefficients with Reynolds number for various surface conditions. $\alpha = 0°$; NACA 66(218)-420 airfoil, 8-foot chord.
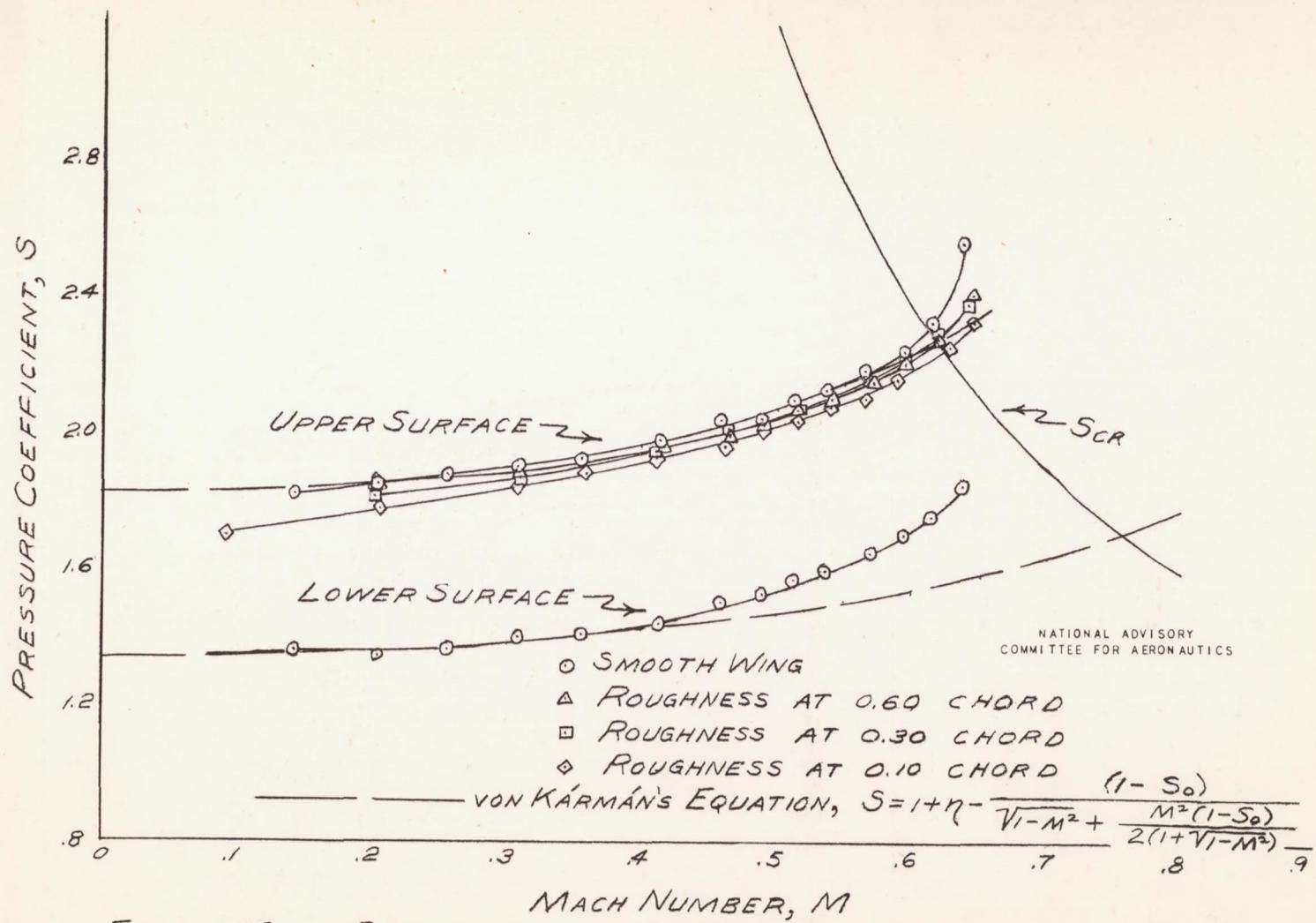
FIGURE 13. — EFFECT OF COMPRESSIBILITY AND SURFACE CONDITION ON THE MINIMUM PRESSURE COEFFICIENTS. $\alpha = 0°$; NACA 66(218)-420 AIRFOIL, 8-FOOT CHORD.
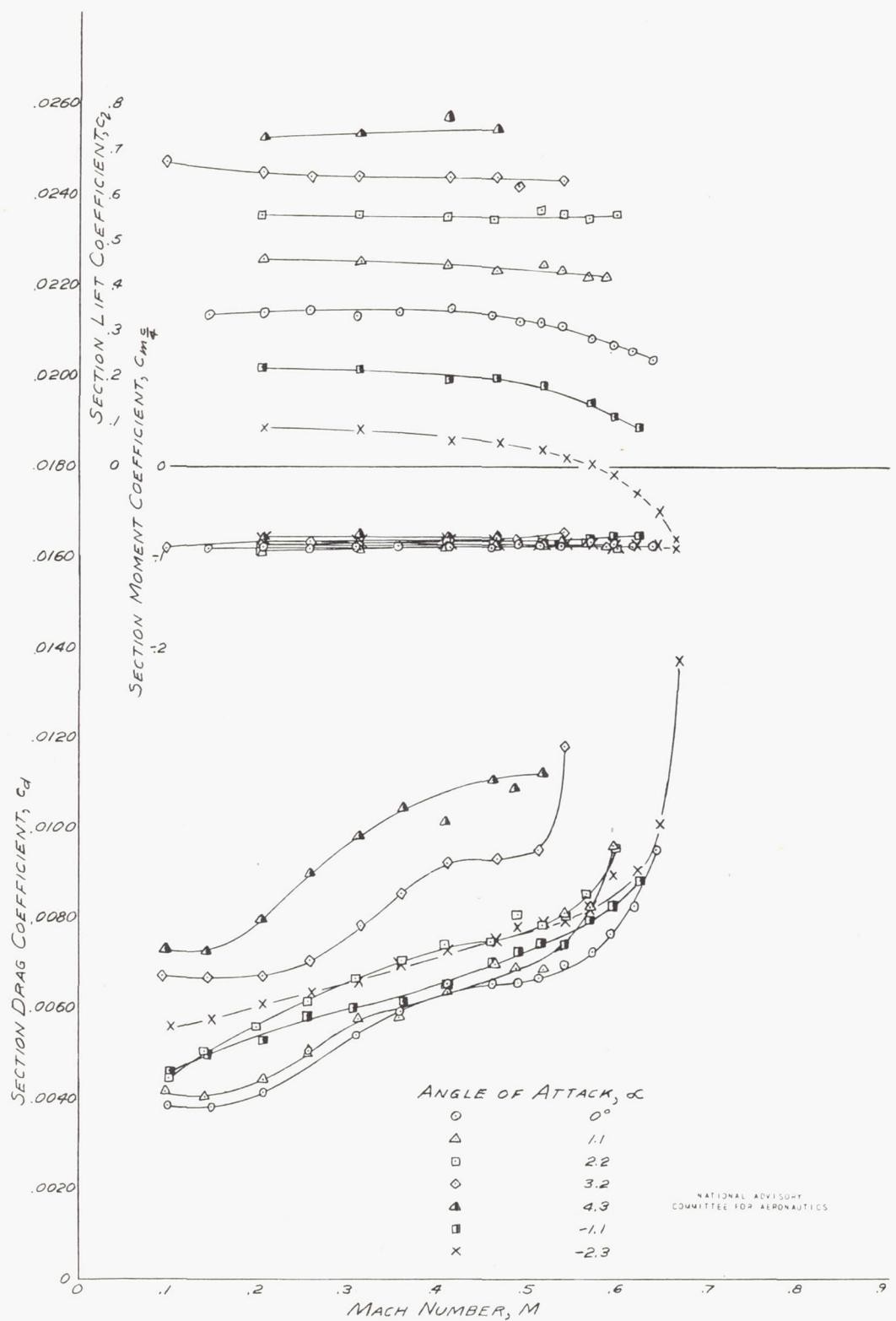
FIGURE 14. - VARIATION OF THE SECTION COEFFICIENTS WITH MACH
NUMBER AND ANGLE OF ATTACK.
NACA 66(2/8)-420 AIRFOIL, 8-FOOT CHORD
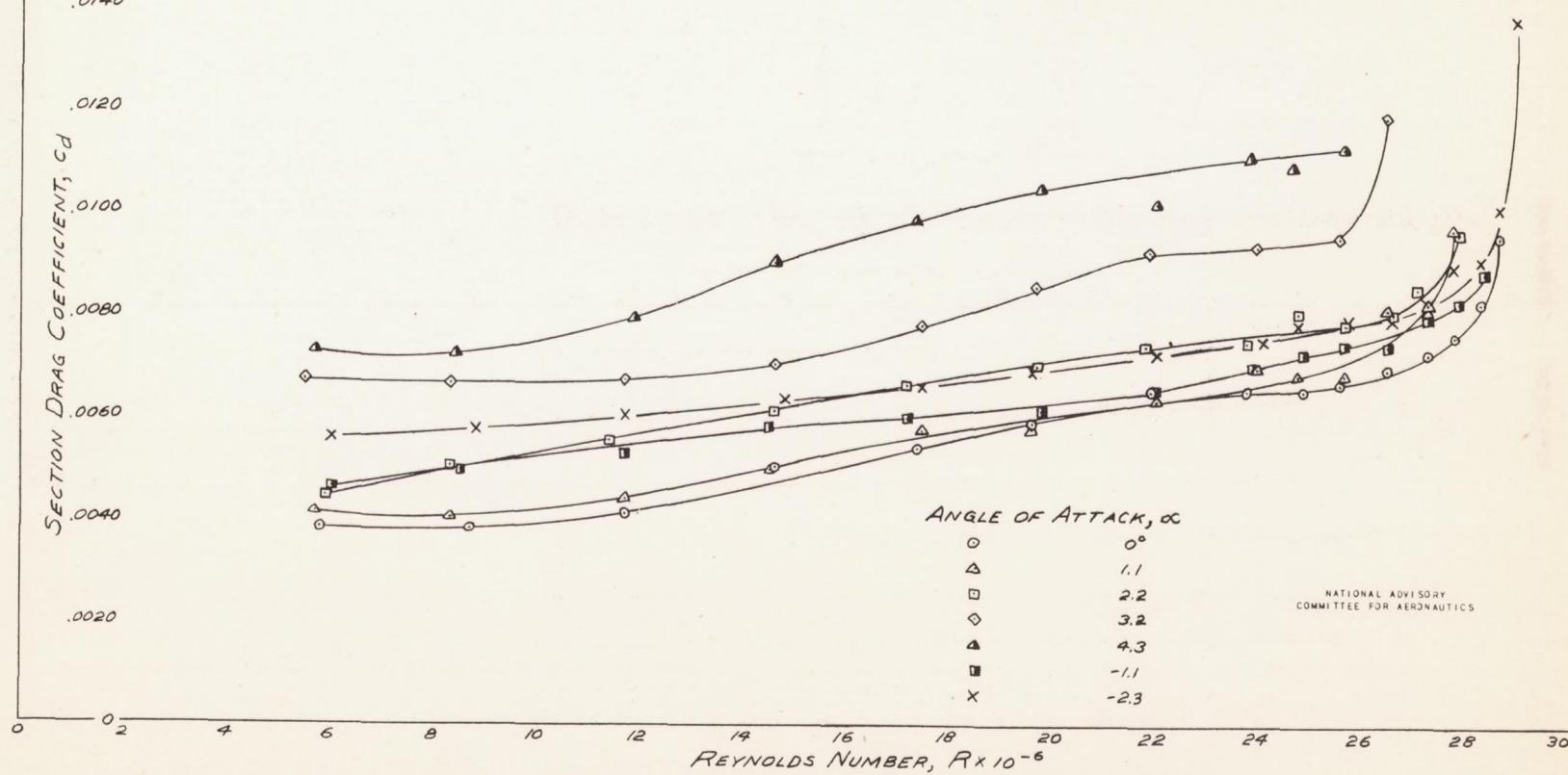
FIGURE 15(a). - VARIATION OF THE SECTION DRAG COEFFICIENT WITH REYNOLDS NUMBER AND ANGLE OF ATTACK. NACA 66(218)-420 AIRFOIL, 8-FOOT CHORD.
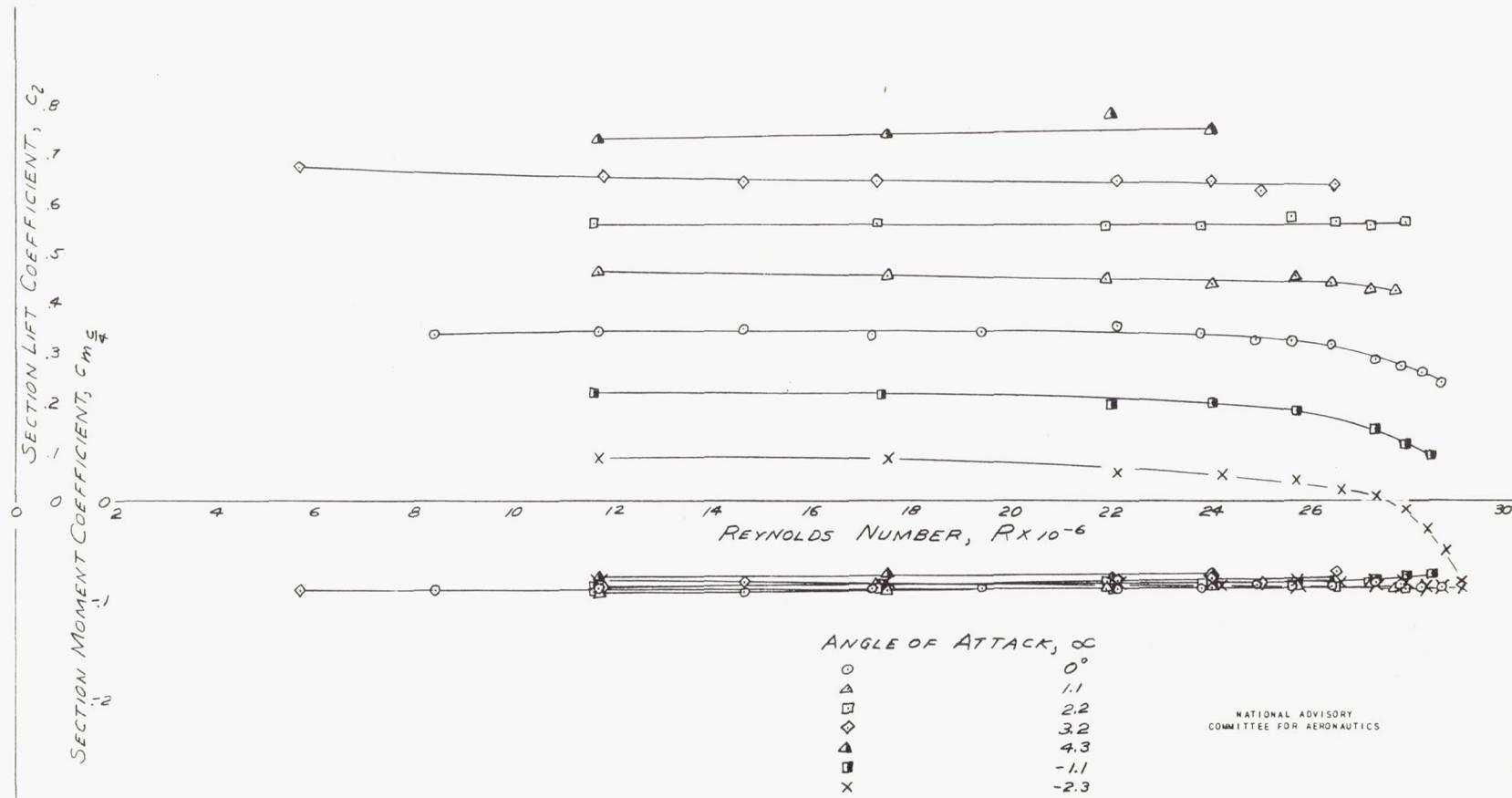
FIGURE 15(b). - VARIATION OF THE SECTION LIFT AND PITCHING MOMENT COEFFICIENTS
WITH REYNOLDS NUMBER AND ANGLE OF ATTACK.
NACA 66(218)-420 AIRFOIL, 8-FOOT CHORD.
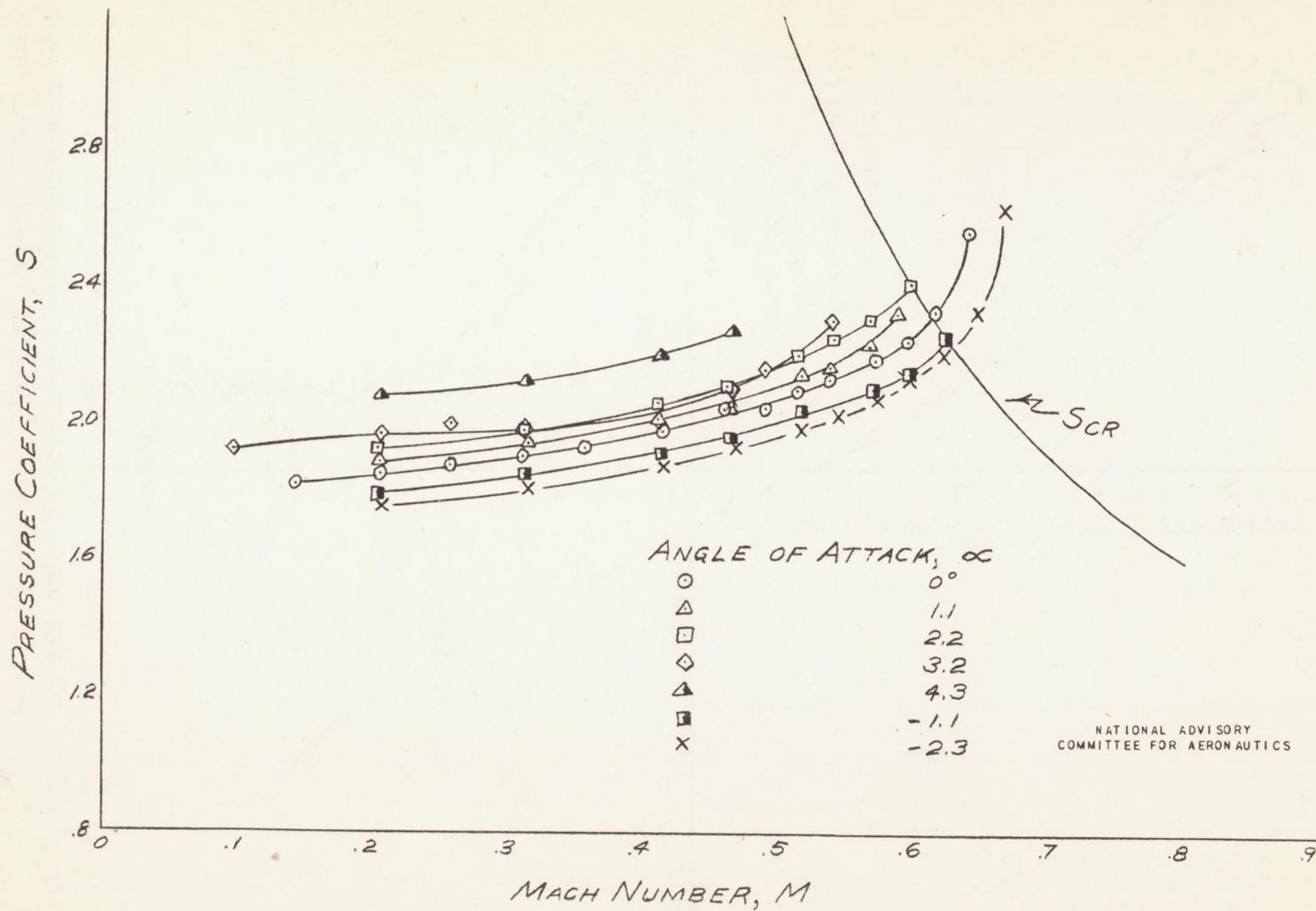
FIGURE 16. – EFFECT OF COMPRESSIBILITY AND ANGLE OF ATTACK ON
THE MINIMUM PRESSURE COEFFICIENT OF THE UPPER SURFACE.
NACA 66(218)-420 AIRFOIL, 8-FOOT CHORD.
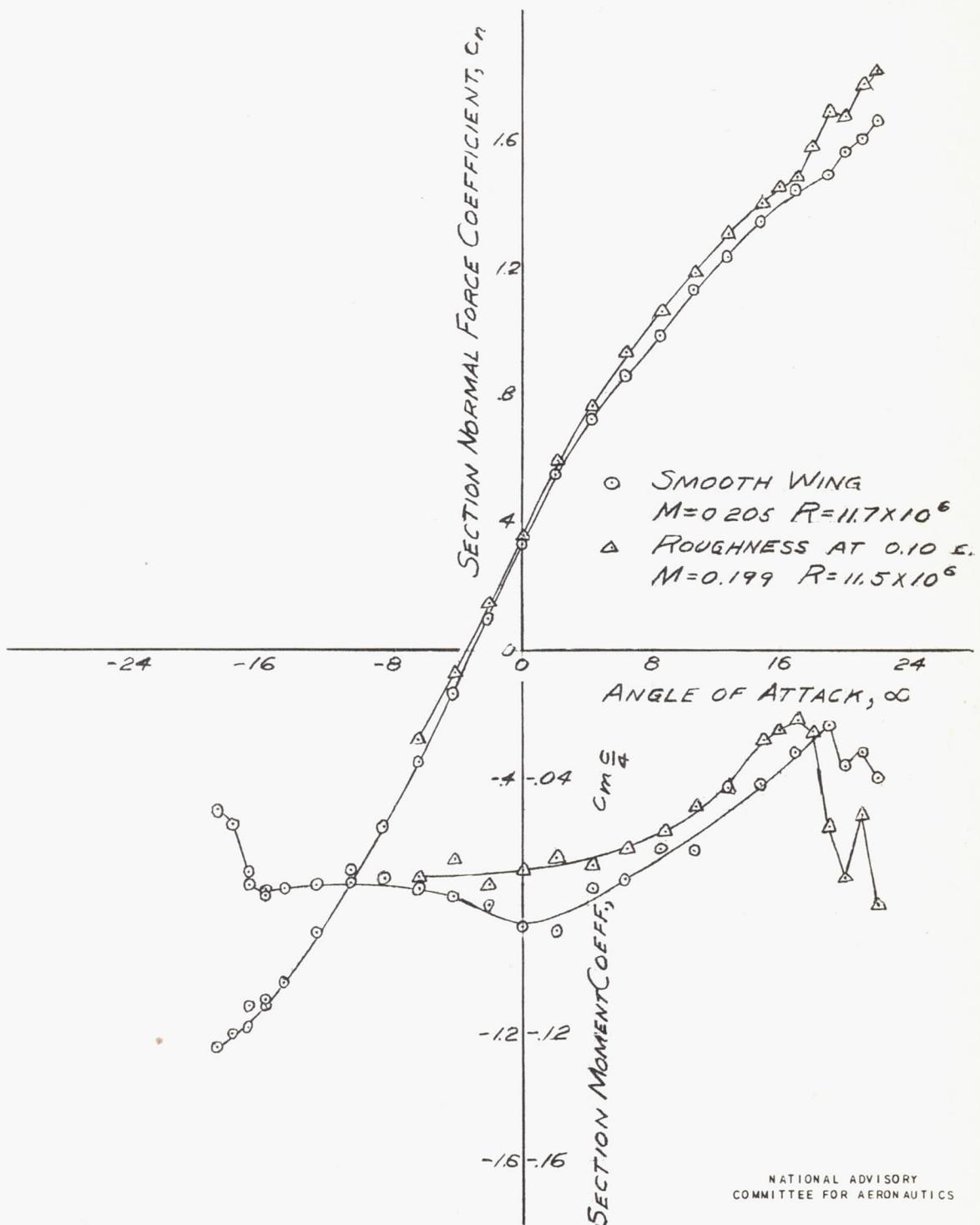
FIGURE 17. - VARIATION OF SECTION COEFFICIENTS WITH
ANGLE OF ATTACK THROUGH STALL CONDITION.
NACA 66(218)-420 AIRFOIL, 8-FOOT CHORD.

Section Lift Coefficient, c_l

Section Moment Coefficient, $c_{m_{c/4}}$

.0260
.6
.5
.4
.0240
.3
.2
.0220
.1
.0200
0

.0180
.1

.0160

.2

.0140

Section Drag Coefficient, c_d

.0120

.0010

.0080

.0060

.0040

○ SMOOTH WING
△ ROUGHNESS AT 0.50 CHORD
□ ROUGHNESS AT 0.30 CHORD
◇ ROUGHNESS AT 0.10 CHORD

NATIONAL ADVISORY
COMMITTEE FOR AERONAUTICS

.0020

0

0   .1   .2   .3   .4   .5   .6   .7   .8   .9
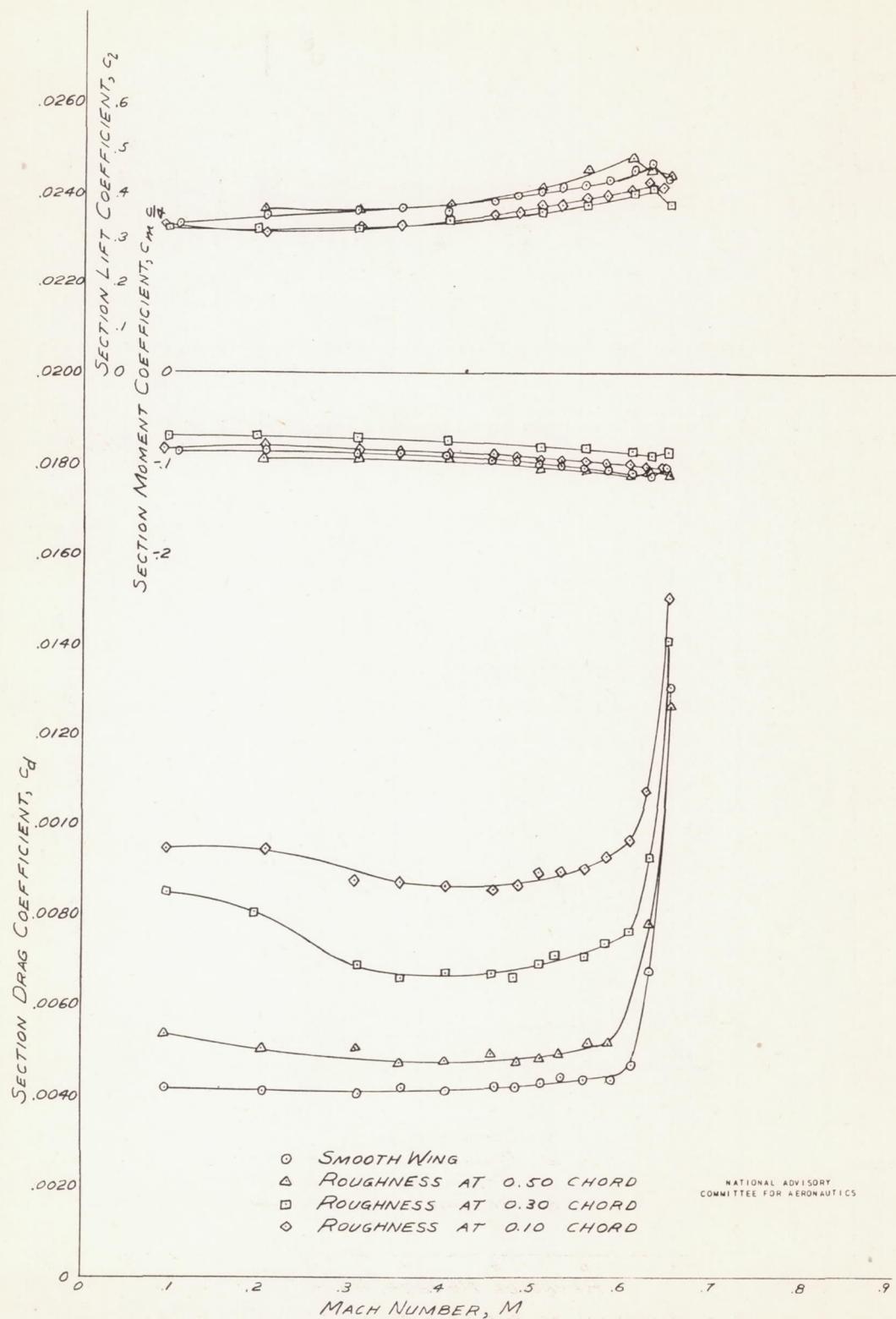
MACH NUMBER, M

FIGURE 18.-VARIATION OF THE SECTION COEFFICIENTS WITH MACH
NUMBER FOR VARIOUS SURFACE CONDITIONS. $\alpha = 0°$,
NACA 65(216)-420 AIRFOIL, 5-FOOT CHORD.

○   SMOOTH WING
△   ROUGHNESS AT 0.50 CHORD
□   ROUGHNESS AT 0.30 CHORD
◇   ROUGHNESS AT 0.10 CHORD
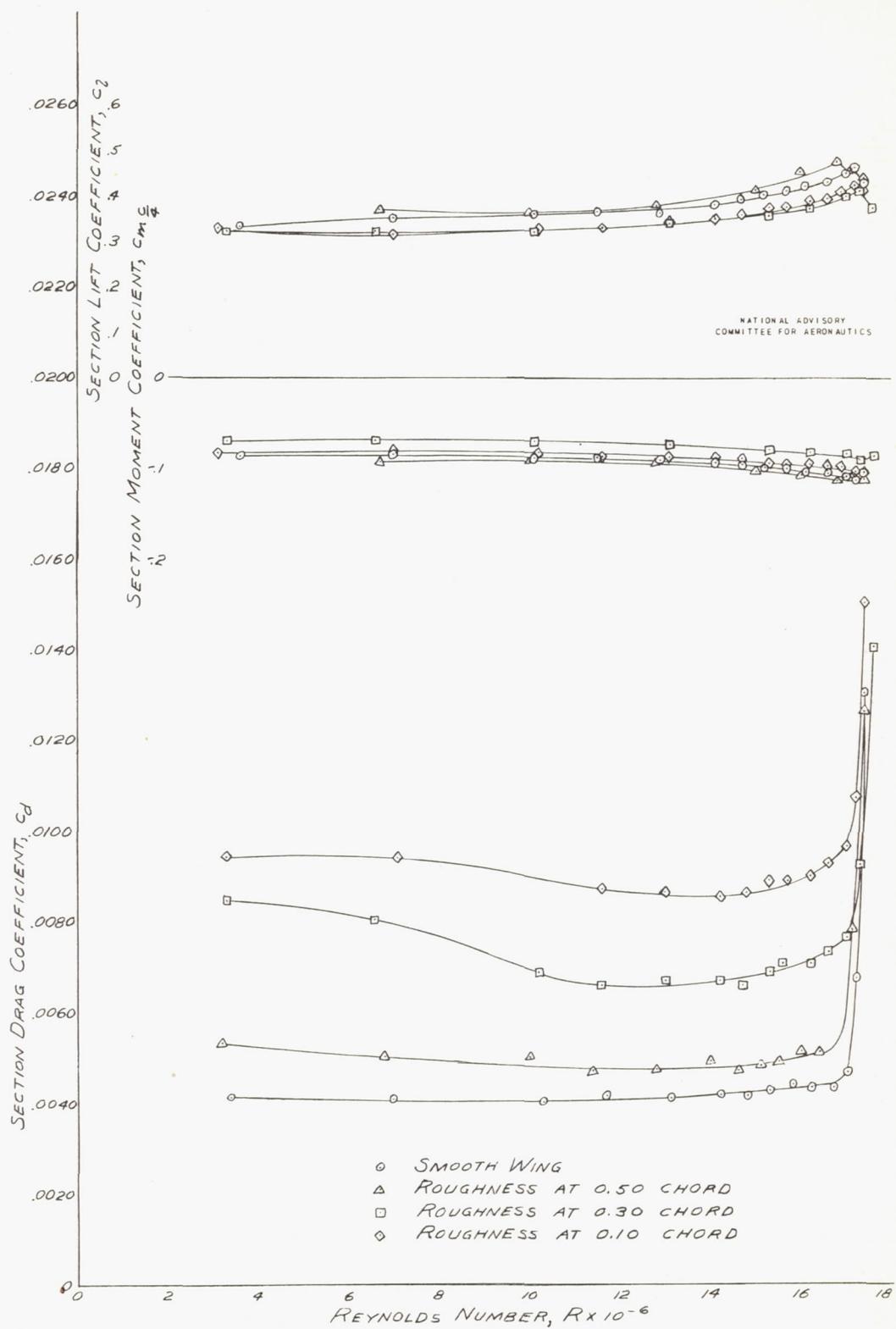
FIGURE 19. – VARIATION OF THE SECTION COEFFICIENTS WITH REYNOLDS NUMBER FOR VARIOUS SURFACE CONDITIONS. $\alpha = 0°$, NACA 65(216)-420 AIRFOIL, 5-FOOT CHORD.
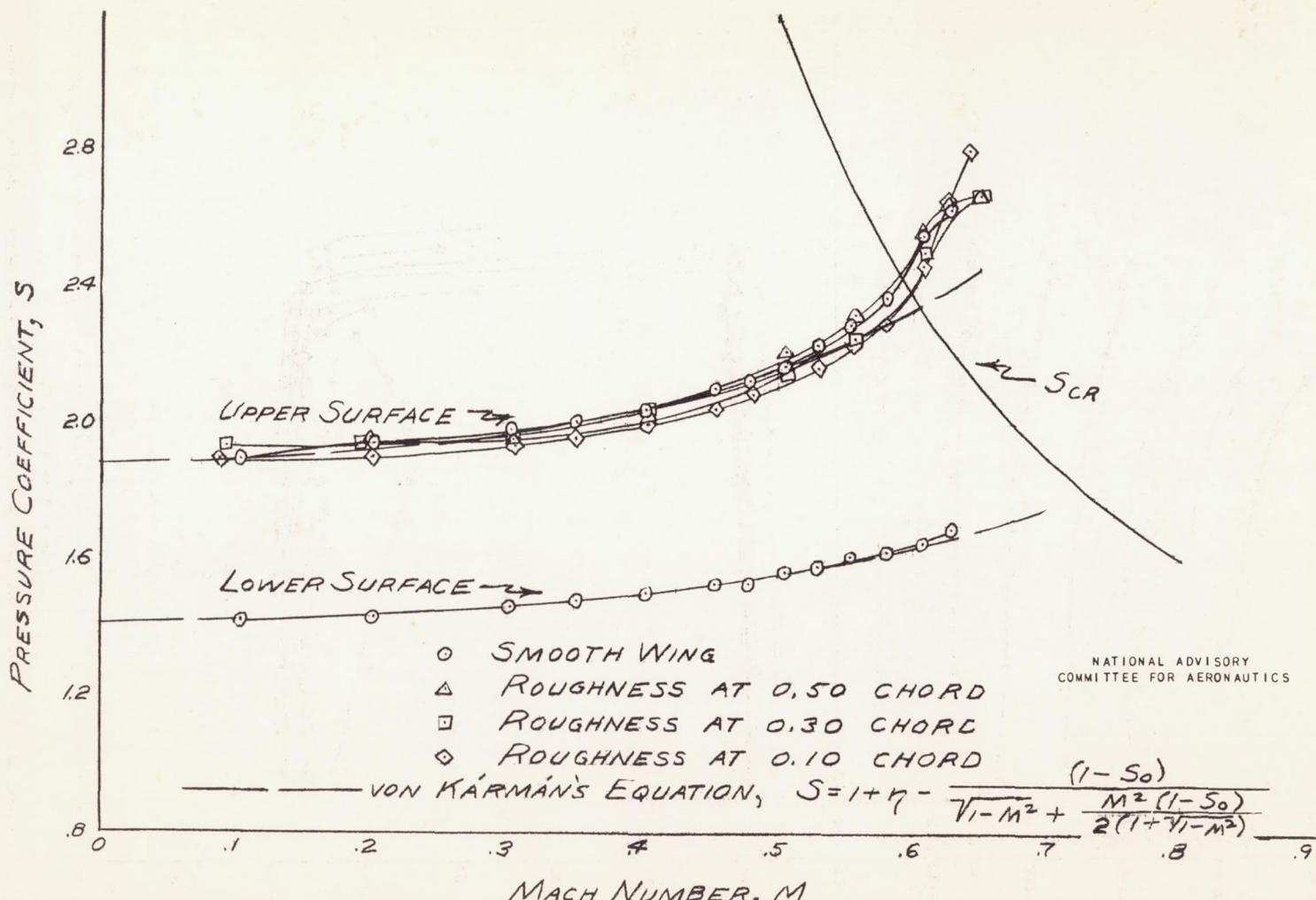
FIGURE 20. – EFFECT OF COMPRESSIBILITY AND SURFACE CONDITION ON THE MINIMUM PRESSURE COEFFICIENTS. $\alpha = 0°$, NACA 65(216)–420 AIRFOIL, 5-FOOT CHORD.
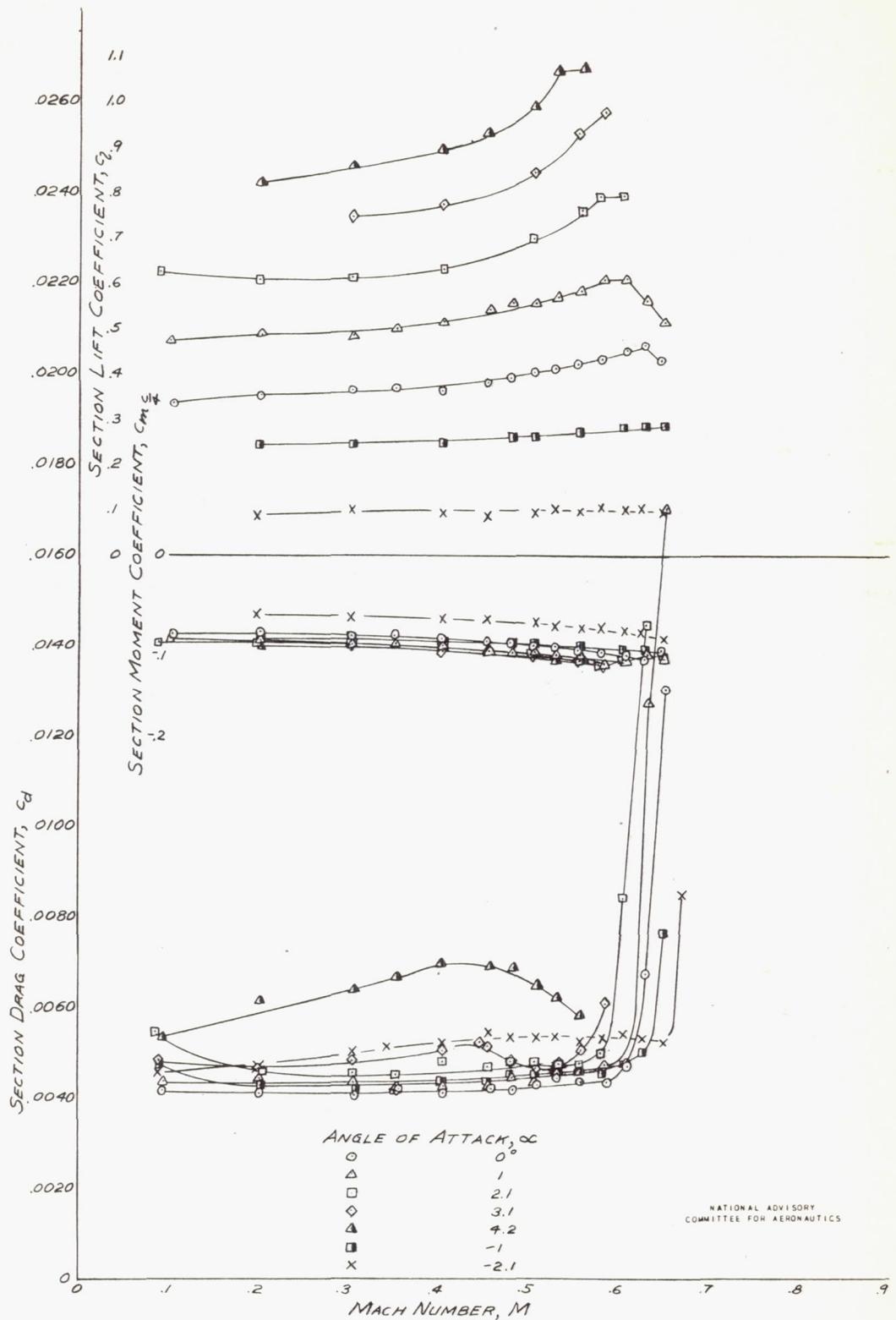
FIGURE 21. — VARIATION OF THE SECTION COEFFICIENTS WITH MACH NUMBER AND ANGLE OF ATTACK. NACA 65(216)-420 AIRFOIL, 5-FOOT CHORD.
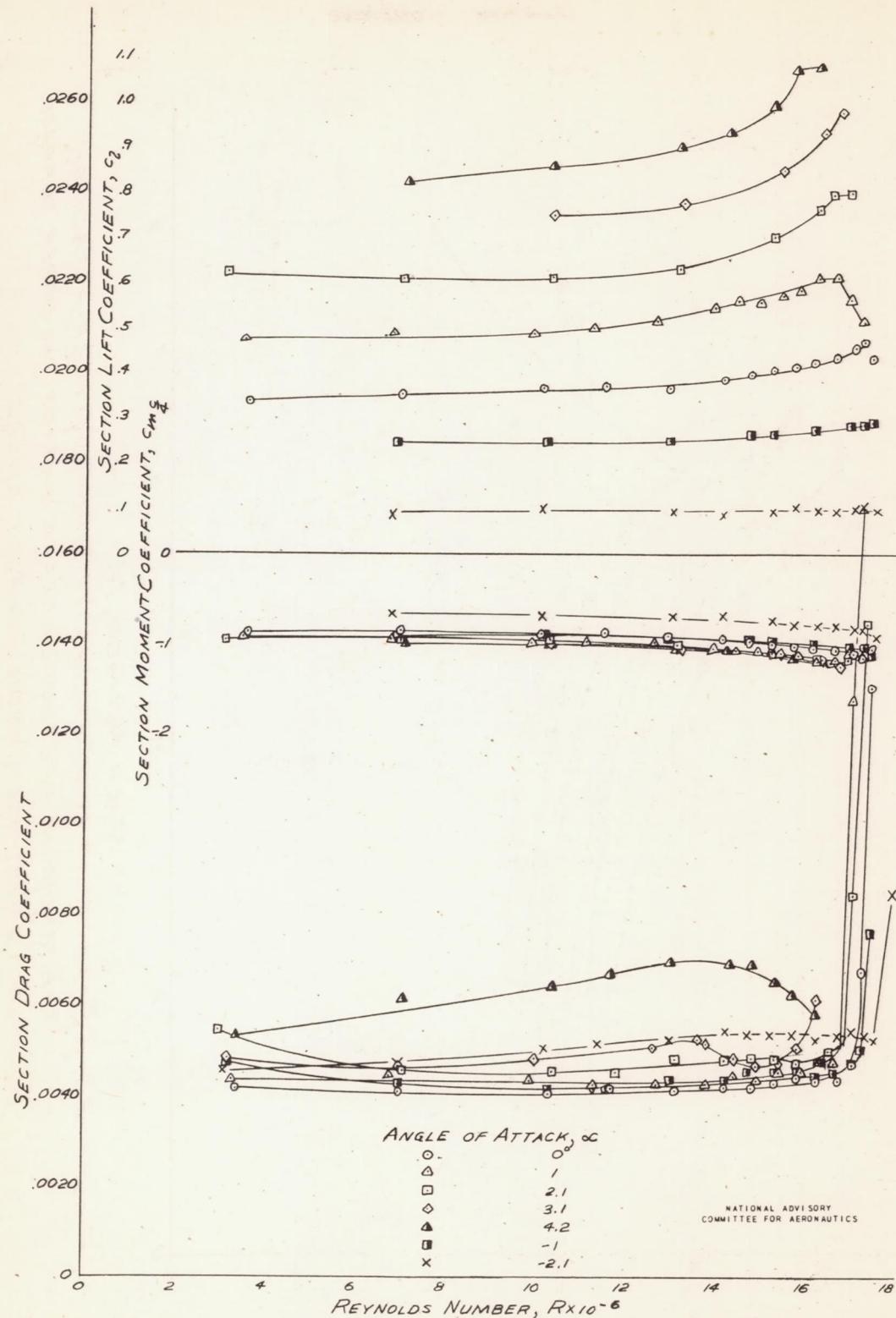
FIGURE 22. - VARIATION OF THE SECTION COEFFICIENTS WITH REYNOLDS NUMBER AND ANGLE OF ATTACK. NACA 65(216)-920 AIRFOIL, 5-FOOT CHORD.

NATIONAL ADVISORY
COMMITTEE FOR AERONAUTICS
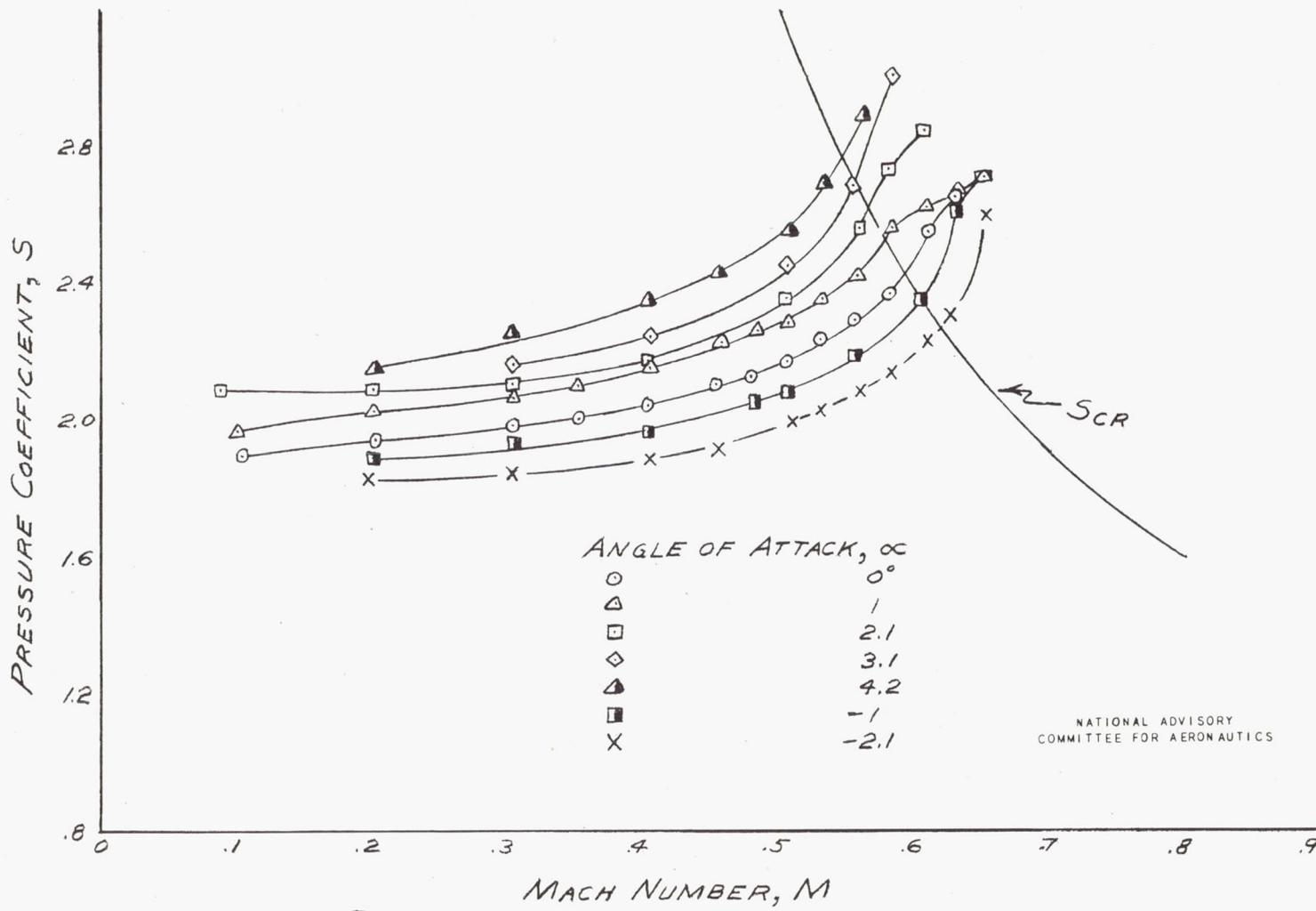
FIGURE 23. — EFFECT OF COMPRESSIBILITY AND ANGLE OF ATTACK ON
THE MINIMUM PRESSURE COEFFICIENT OF THE UPPER SURFACE.
NACA 65(216)-420 AIRFOIL, 5-FOOT CHORD.
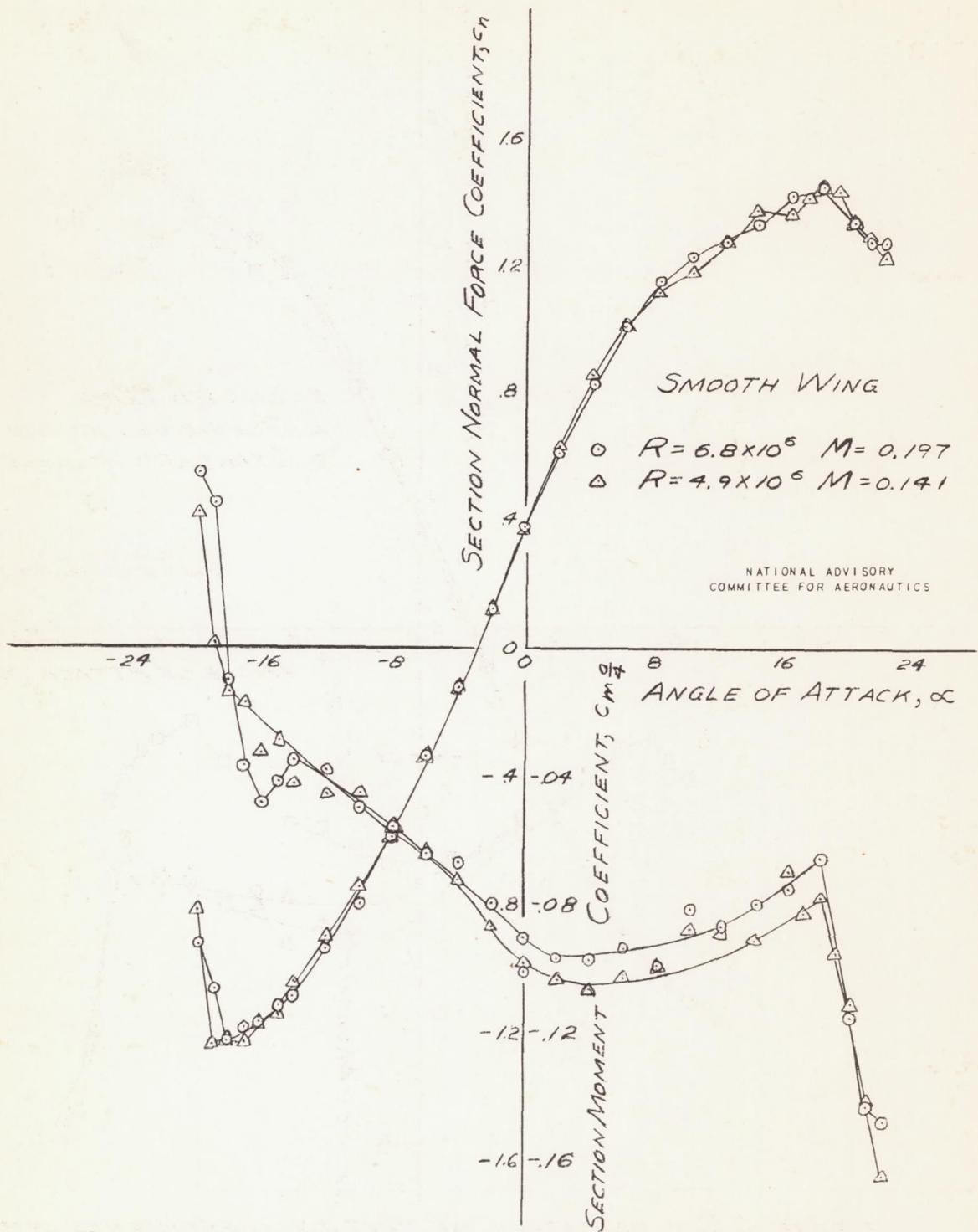
FIGURE 24. - VARIATION OF SECTION COEFFICIENTS WITH
ANGLE OF ATTACK AND REYNOLDS NUMBER THROUGH THE
STALL CONDITION. NACA 65(216)-420 AIRFOIL, 5-FOOT CHORD
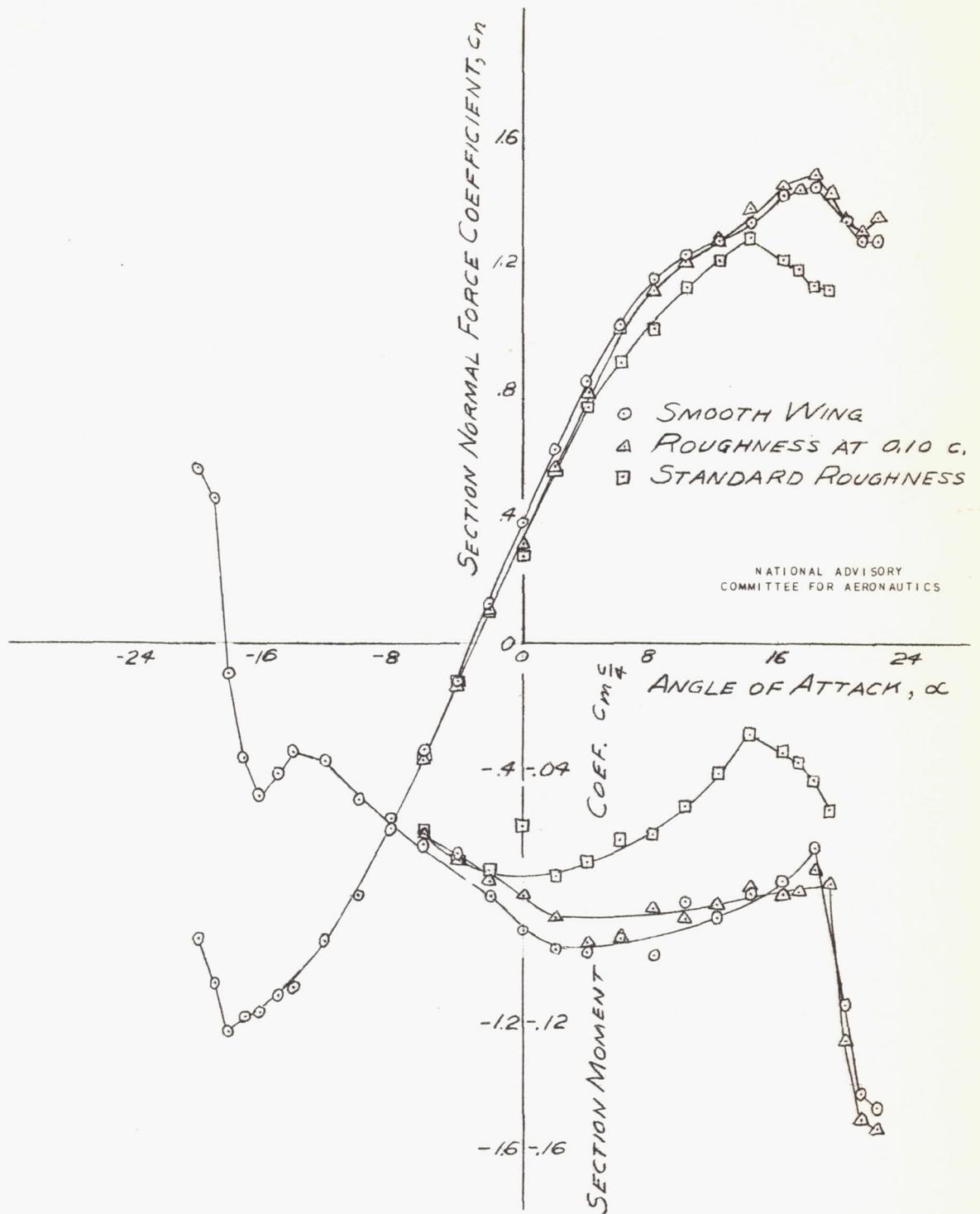
FIGURE 25. – VARIATION OF SECTION COEFFICIENTS WITH ANGLE OF ATTACK FOR SEVERAL SURFACE CONDITIONS. NACA 65(216)-420 AIRFOIL, 5-FOOT CHORD, M=0.195, R=6.8×10⁶
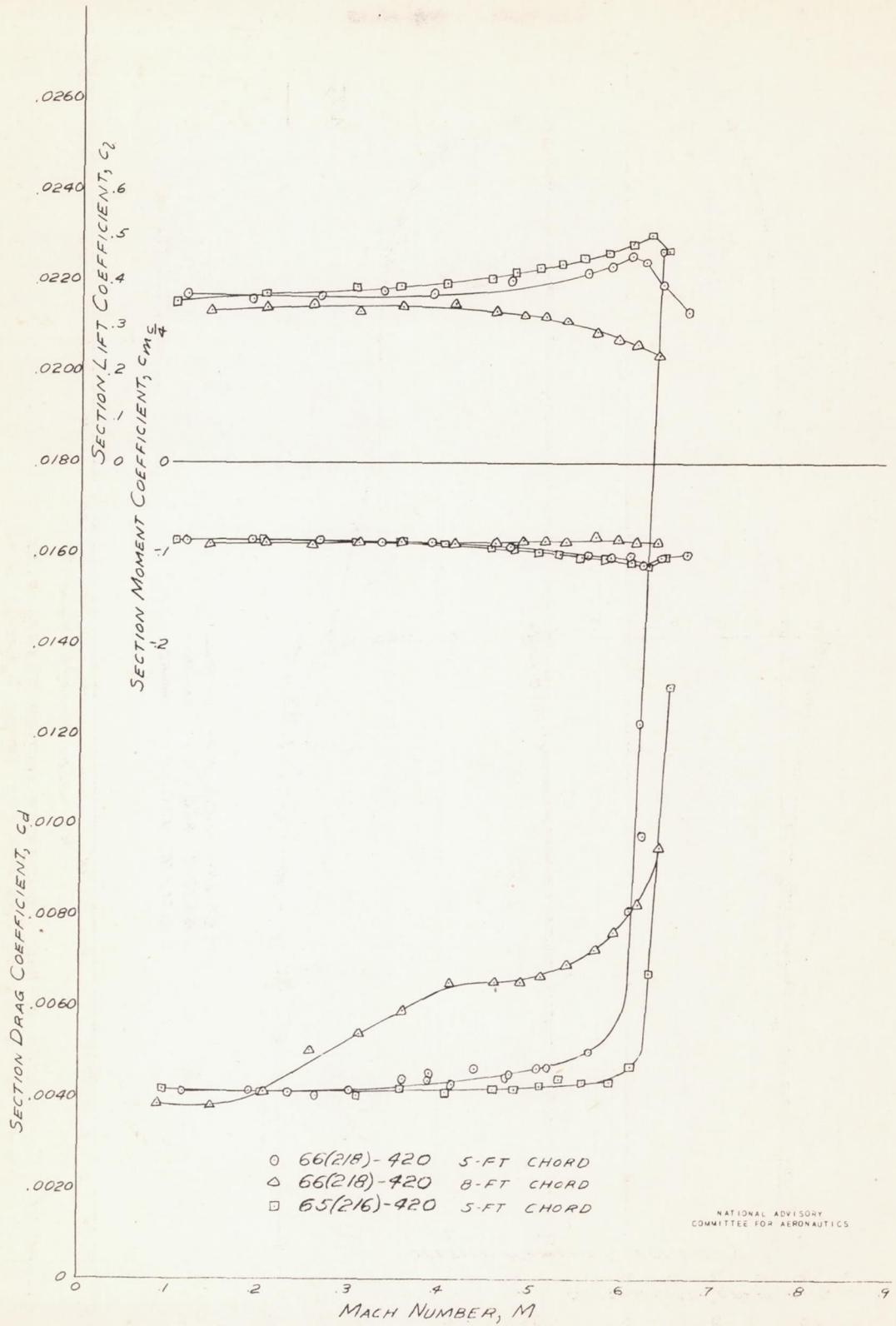
FIGURE 2.6.- COMPARISON OF THE VARIATION OF SECTION COEFFICIENTS
WITH MACH NUMBER FOR THE THREE AIRFOILS. $\alpha = 0°$
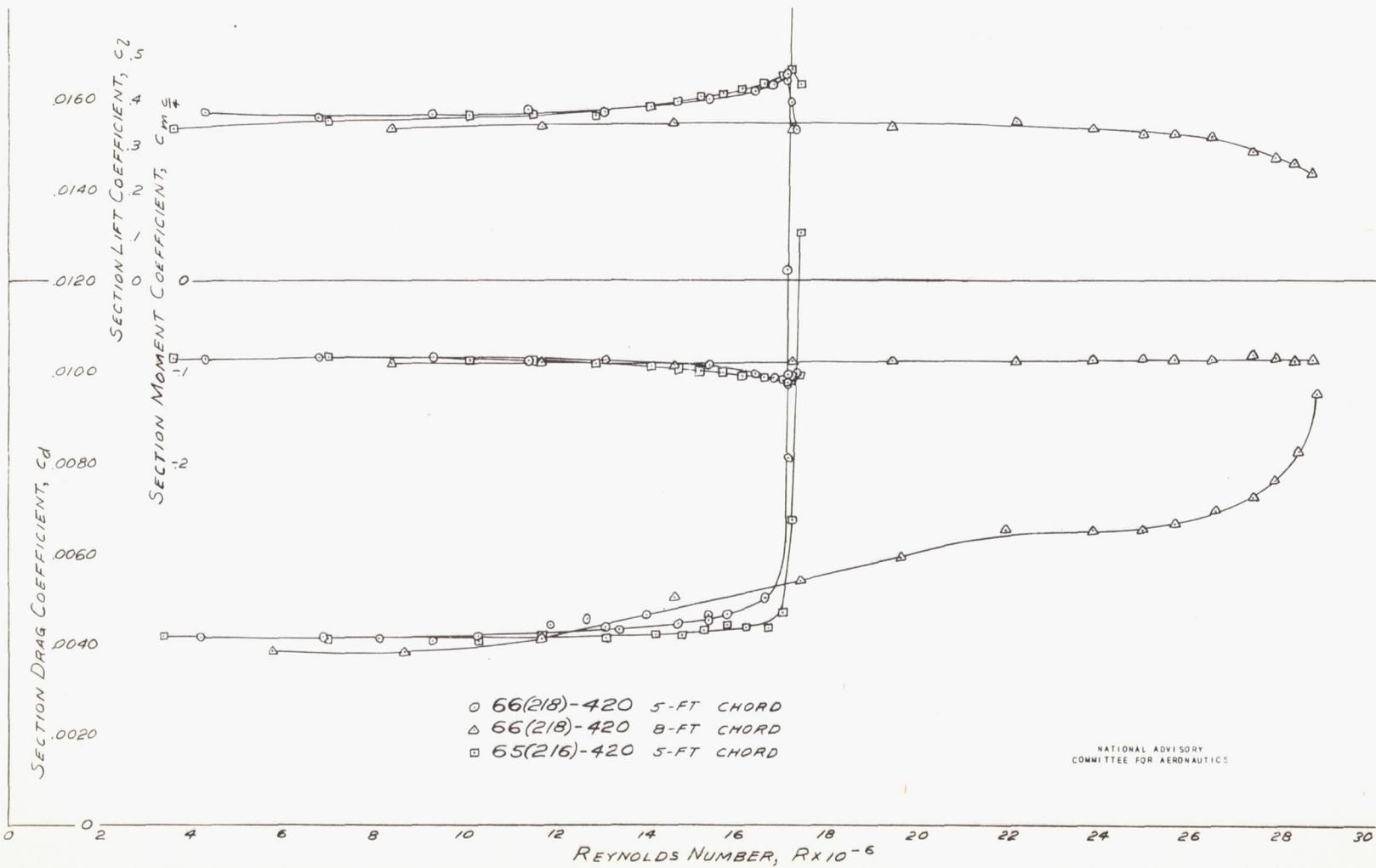
FIGURE 27. - COMPARISON OF THE VARIATION OF SECTION COEFFICIENTS
WITH REYNOLDS NUMBER FOR THE THREE AIRFOILS. $\alpha = 0°$
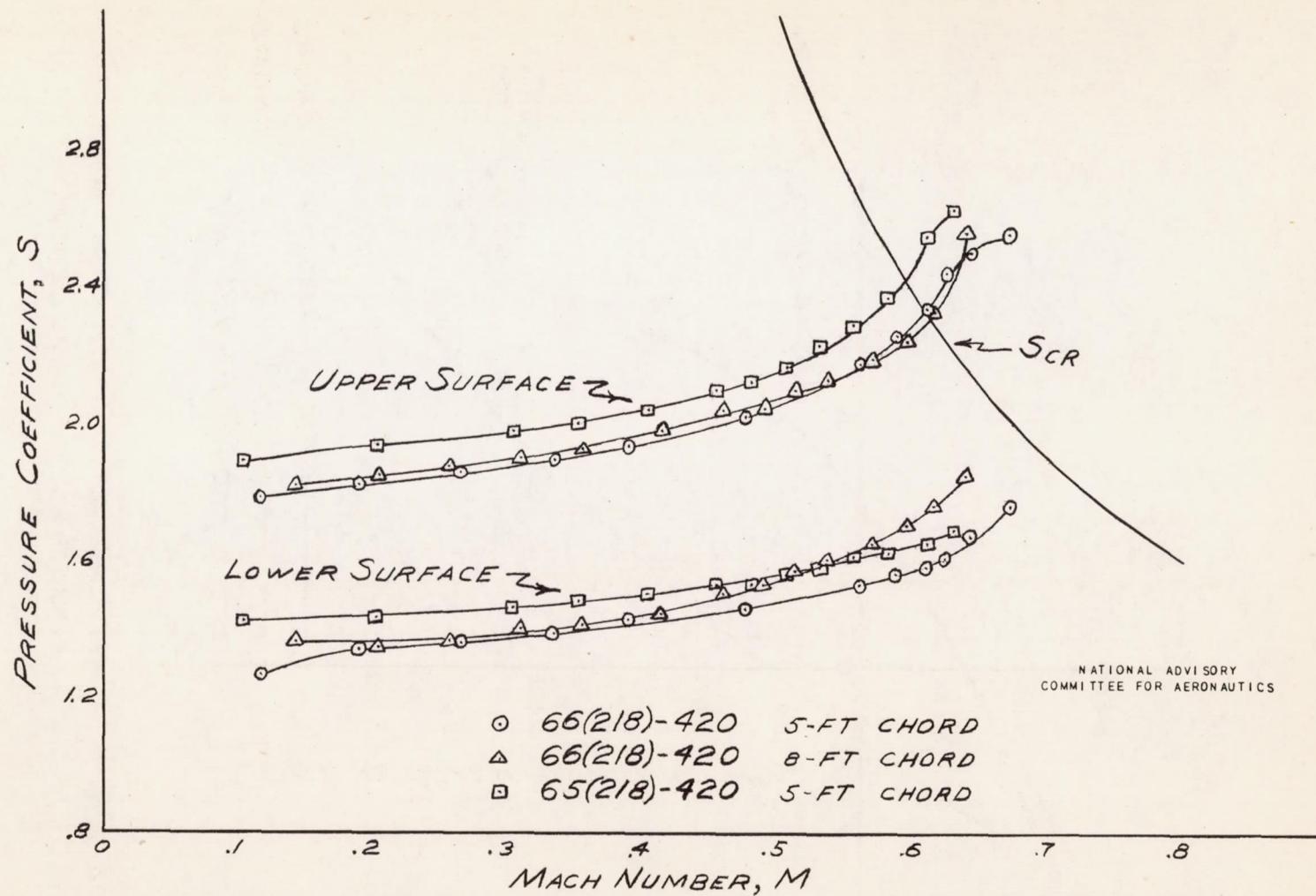
FIGURE 28.- COMPARISON OF THE MINIMUM PRESSURE COEFFICIENTS
FOR THE THREE AIRFOILS, ∝=0°
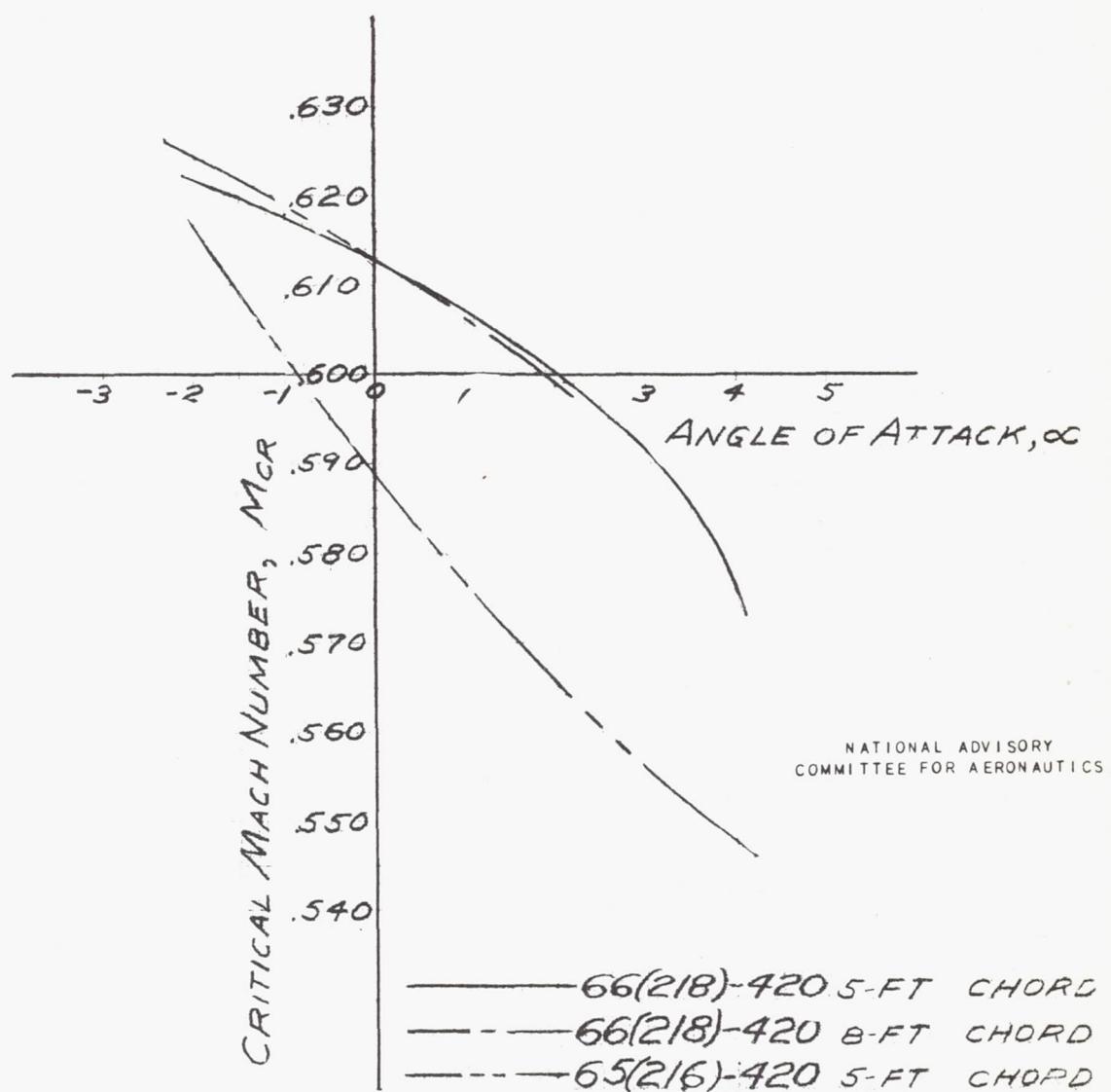
FIGURE 29.- CRITICAL SPEED OF THE AIRFOILS AS A FUNCTION OF ANGLE OF ATTACK.

SECTION LIFT COEFFECIENT AT M_{CR}, $C_{l_{M_{CR}}}$

CRITICAL MACH NUMBER, M_{CR}

NATIONAL ADVISORY
COMMITTEE FOR AERONAUTICS

——————— 66(218)-420 5-FT. CHORD
———·——— 66(218)-420 8-FT. CHORD
———··——— 65(216)-420 5-FT CHORD
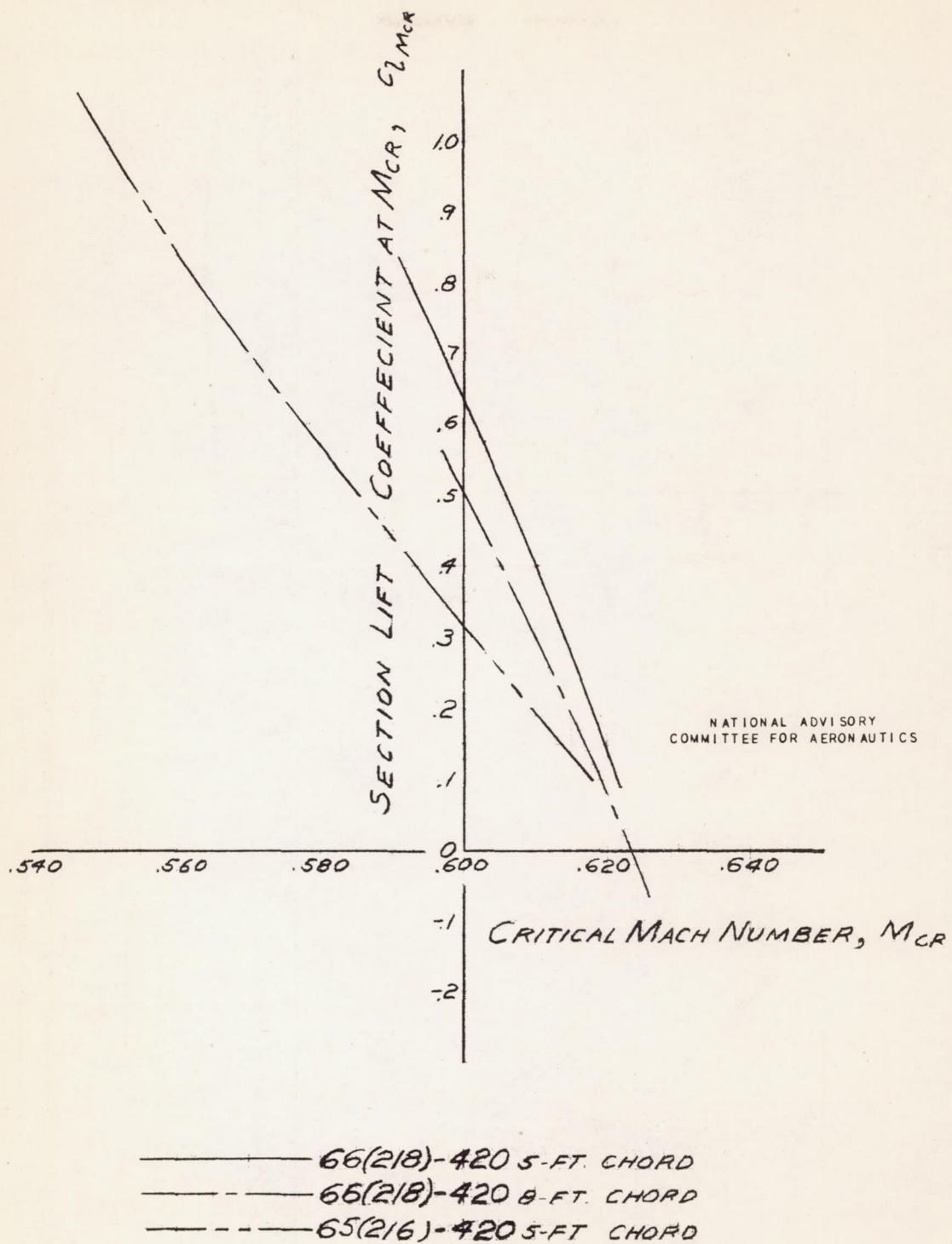
FIGURE 30. - CRITICAL SPEED OF THE AIRFOILS AS
A FUNCTION OF LIFT COEFFICIENT.

Section Lift Coefficient, c_l

Angle of Attack, α

Section Moment Coefficient, $c_{m\frac{c}{4}}$

Section Drag Coefficient, c_d

Section Lift Coefficient, c_l
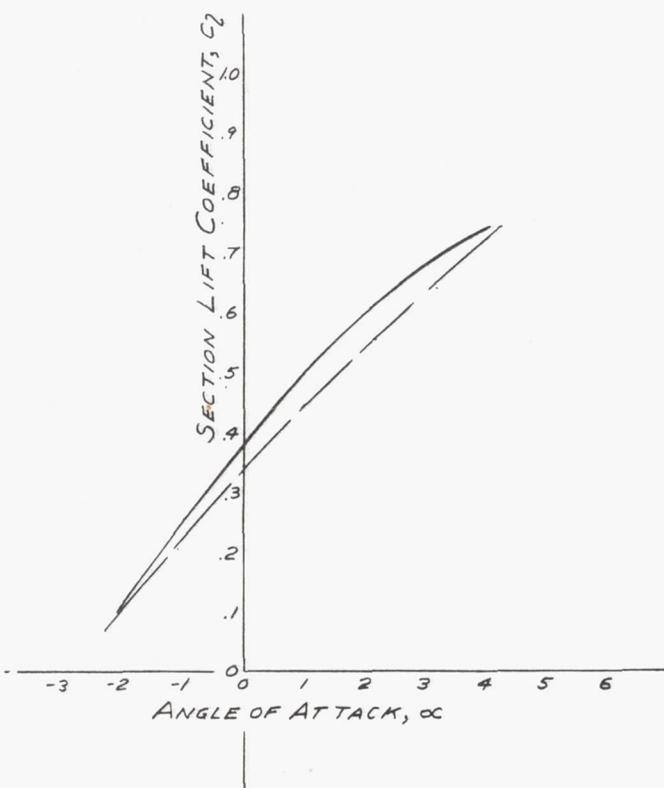
———— 5-FT CHORD $R = 12.9 \times 10^6$

— — — 8-FT CHORD $R = 22.0 \times 10^6$
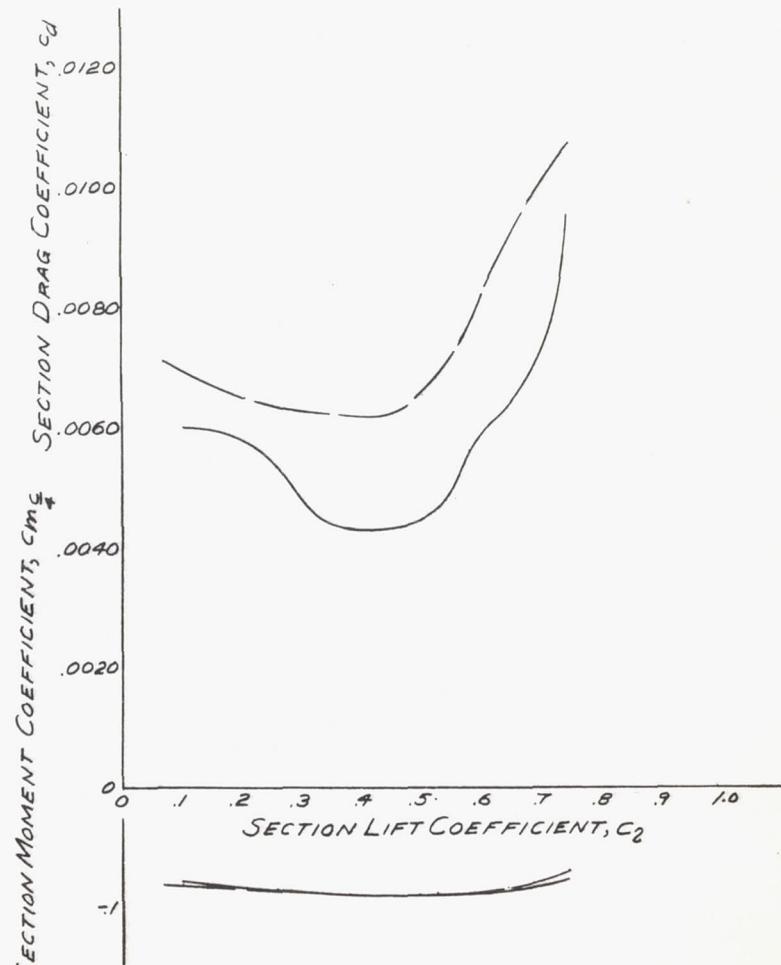
FIGURE 31. - COMPARISON OF THE NACA 66(218)-420 AIRFOILS OF 5-FOOT
AND 8-FOOT CHORD AT M=0.4.

5-FT CHORD   M = 0.440
8-FT CHORD   M = 0.250

NATIONAL ADVISORY
COMMITTEE FOR AERONAUTICS
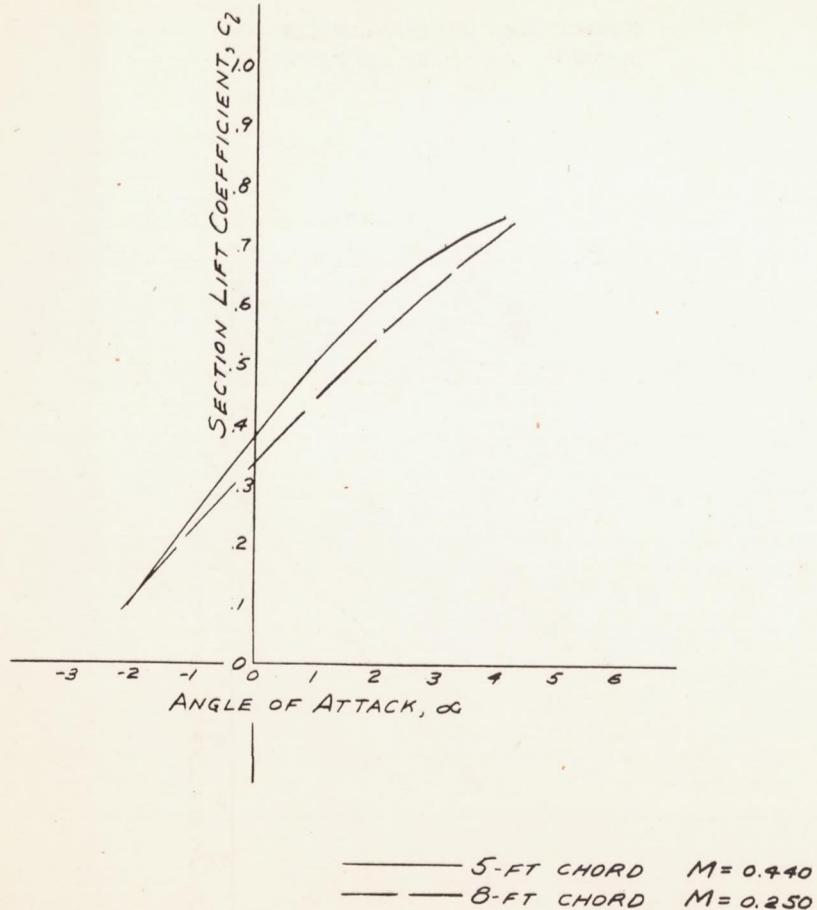
FIGURE 32. — COMPARISON OF THE NACA 66(218)-420 AIRFOILS OF
5-FOOT AND 8-FOOT CHORD AT $R = 14 \times 10^6$

Figure 33.- Comparison of NACA 66(218)-420 and 65(216)-420 airfoils of 5-foot chord, at M = 0.4 and R = 12.9 X 10⁶.
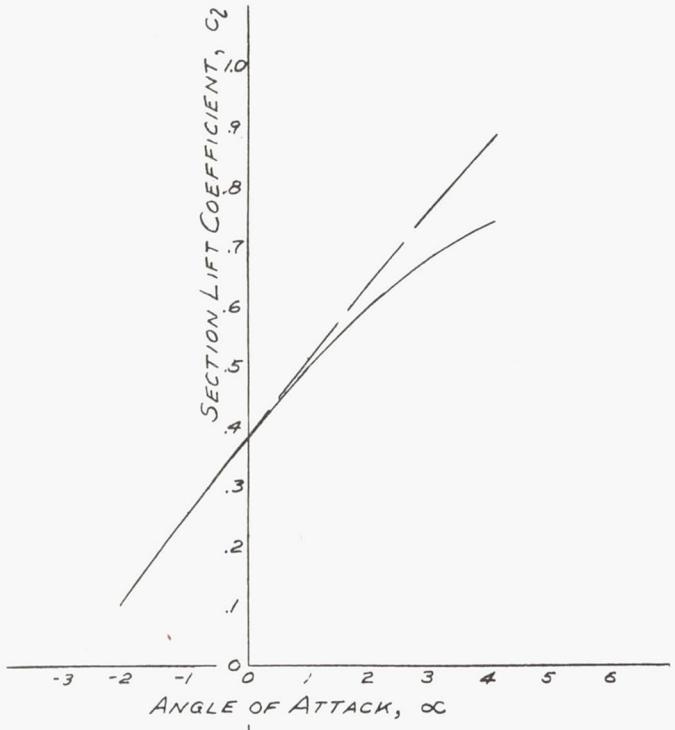
Legend:
————— 66(218)-420 5-FT. CHORD
— — — 65(216)-420 5-FT. CHORD

SECTION NORMAL FORCE COEFFICIENT, c_n

1.6

1.2

.8

SMOOTH WING

.4

⊙ 66(218)-420 5-FT. C.
$R = 6.7 \times 10^6$ $M = 0.189$

△ 66(218)-420 8-FT. C.
$R = 11.7 \times 10^6$ $M = 0.205$

□ 65(216)-420 5-FT. C.
$R = 6.8 \times 10^6$ $M = 0.197$

-24   -16   -8   0   8   16   24

COEF, $c_{m_{c/4}}$

ANGLE OF ATTACK, α

-.4 -.04

1.2 -.12

SECTION MOMENT

1.6 -.16
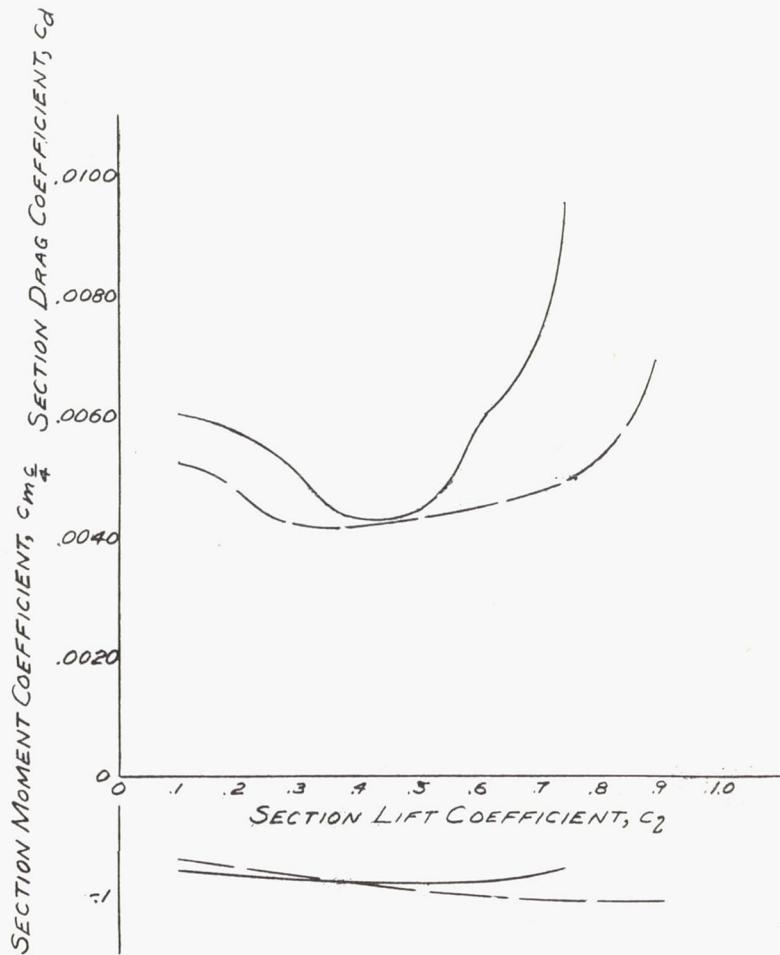
NATIONAL ADVISORY
COMMITTEE FOR AERONAUTICS
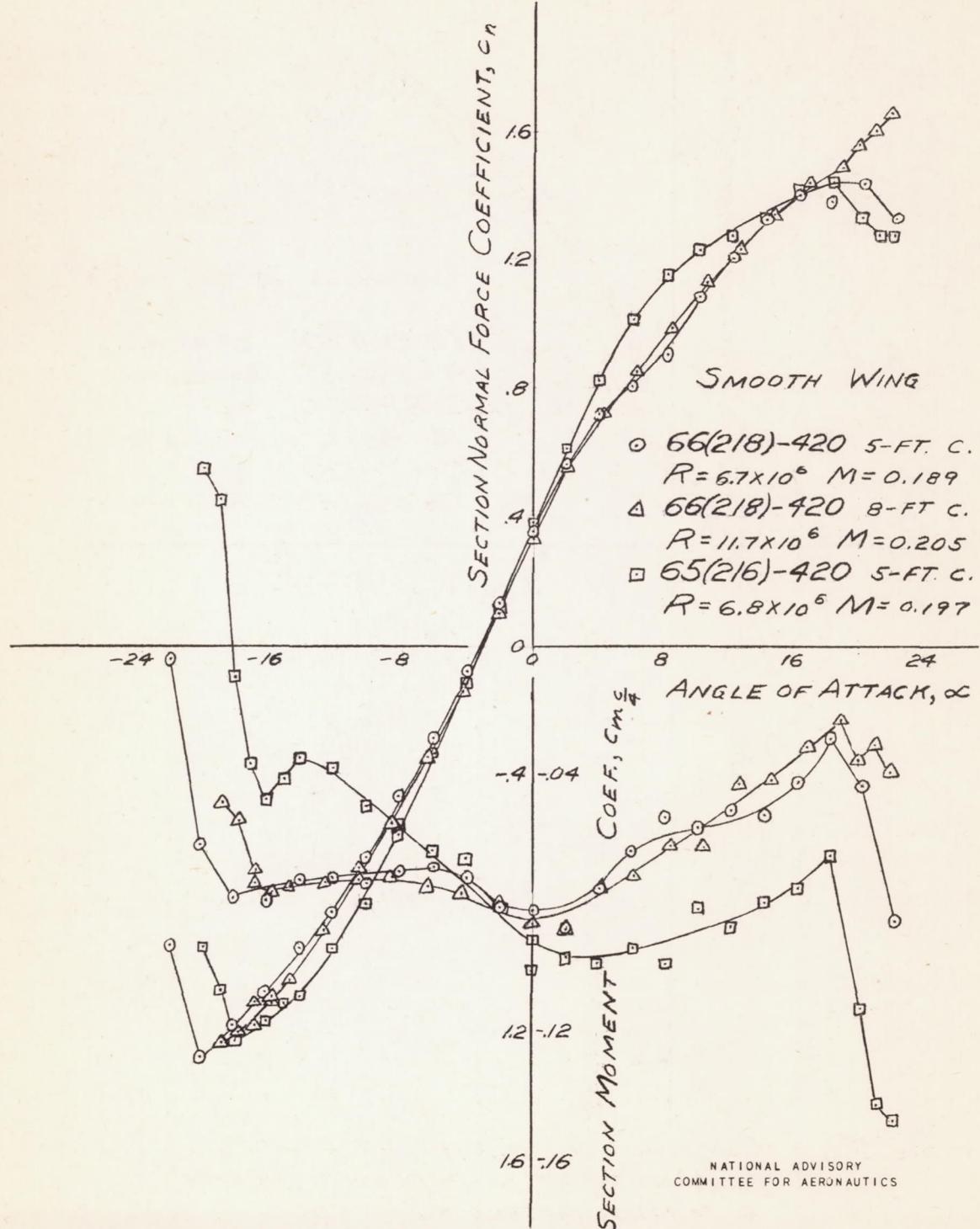
FIGURE 34. - COMPARISON OF THE THREE SMOOTH AIRFOILS
AT ANGLES OF ATTACK THROUGH STALL.
M APPROXIMATELY 0.2
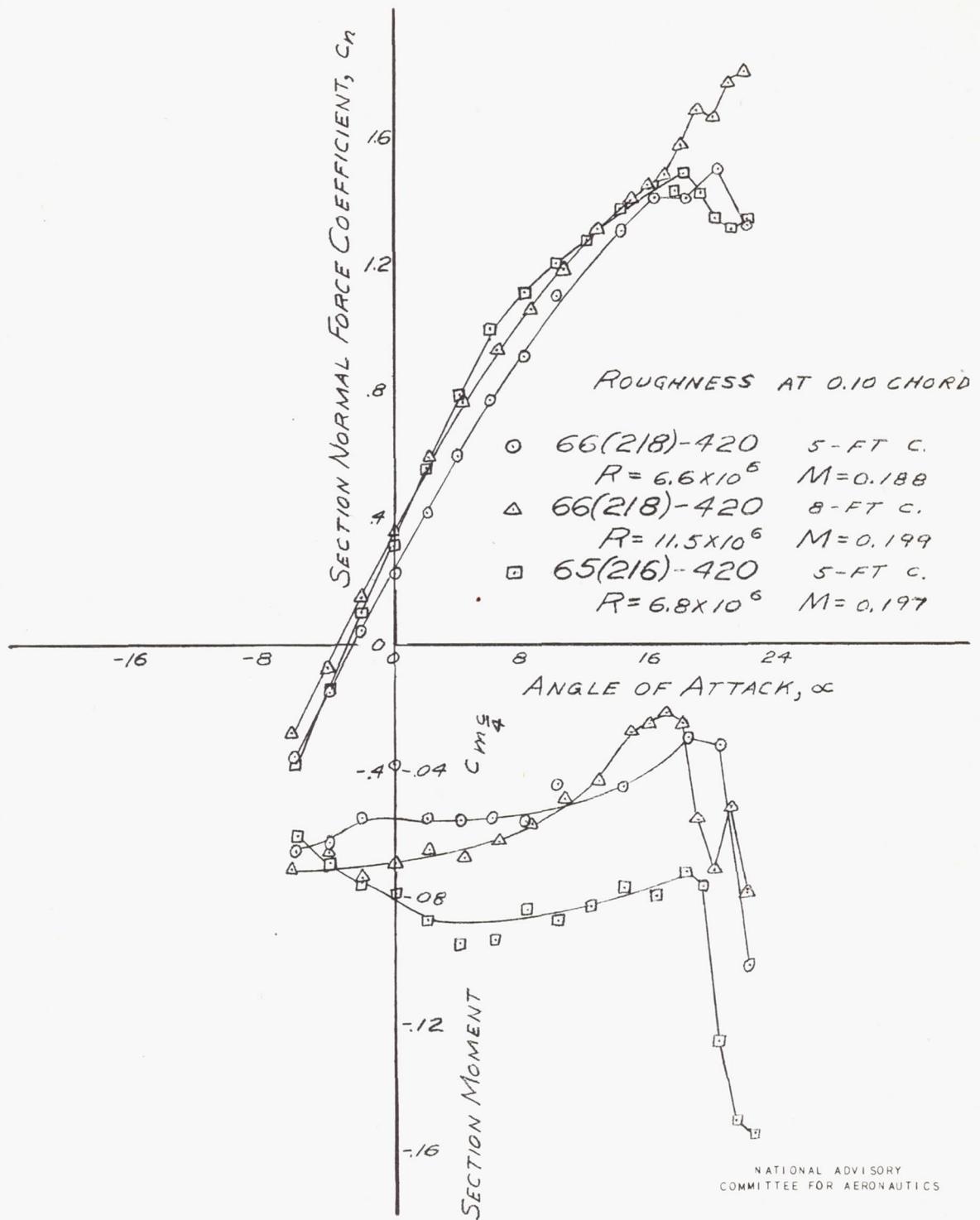
FIGURE 35. — COMPARISON OF THE THREE AIRFOILS WITH ROUGHNESS AT 10-PERCENT CHORD. M APPROXIMATELY 0.2

FIGURE 36. – PRESSURE DISTRIBUTION ON THE SMOOTH NACA 66(218)-420
AIRFOIL. α = 0°, 5-FOOT CHORD.

FIGURE 37. – PRESSURE DISTRIBUTION ON THE SMOOTH NACA 66(218)-420
AIRFOIL. α = 0°, 8-FOOT CHORD.

FIGURE 38.—PRESSURE DISTRIBUTION ON THE NACA 66(218)-420 AIRFOIL
WITH ROUGHNESS AT 10-PERCENT CHORD. α=0°, 5-FOOT CHORD.

MACH NUMBER, M

○	.196
△	.271
☐	.342
◇	.391
▲	.436
◨	.475
◆	.513
◮	.559
⊡	.606
X	.627

NATIONAL ADVISORY
COMMITTEE FOR AERONAUTICS

MACH NUMBER, M

|	
○	.205
△	.313
▢	.413
◇	.467
◭	.515
◧	.543
◈	.570
◮	.595
▢	.620
◈	.644
×	.664

NATIONAL ADVISORY
COMMITTEE FOR AERONAUTICS
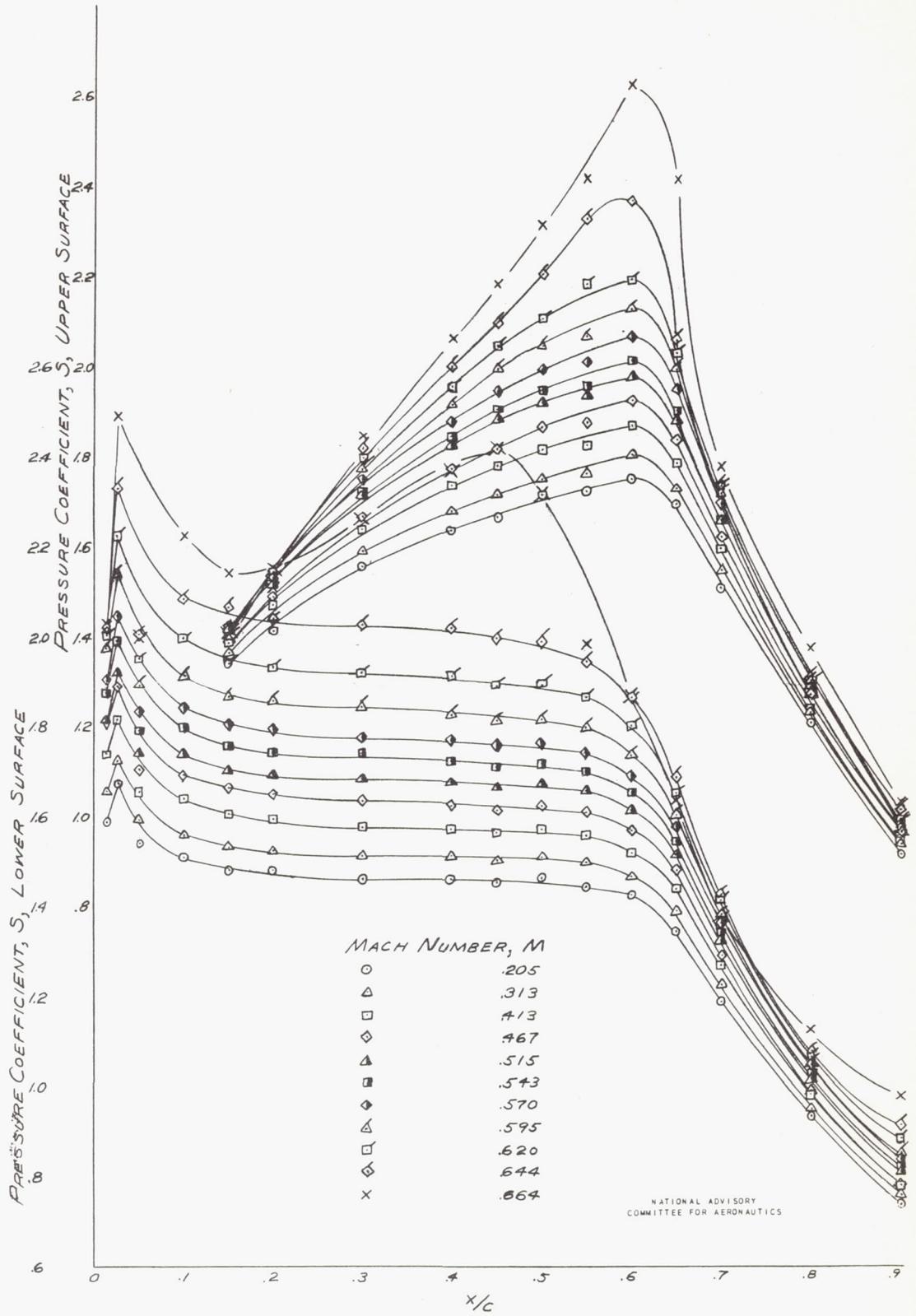
FIGURE 39. - PRESSURE DISTRIBUTION ON THE SMOOTH NACA 66(218)-420
AIRFOIL. $\alpha = -2.3°$, 8-FOOT CHORD.
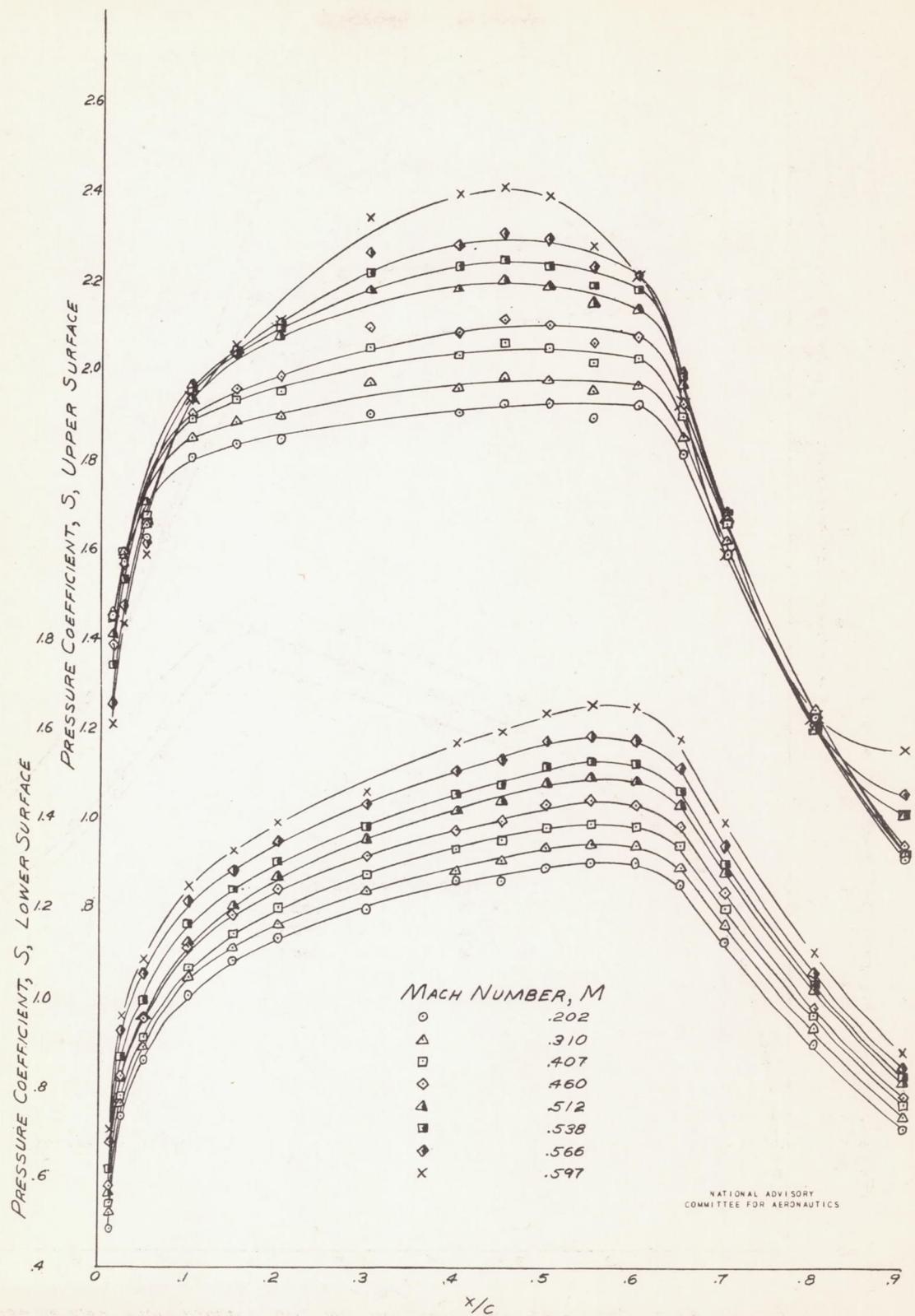
FIGURE 40.– PRESSURE DISTRIBUTION ON THE SMOOTH NACA 66(218)-420 AIRFOIL. ∝ = +2.2°, 8-FOOT CHORD.
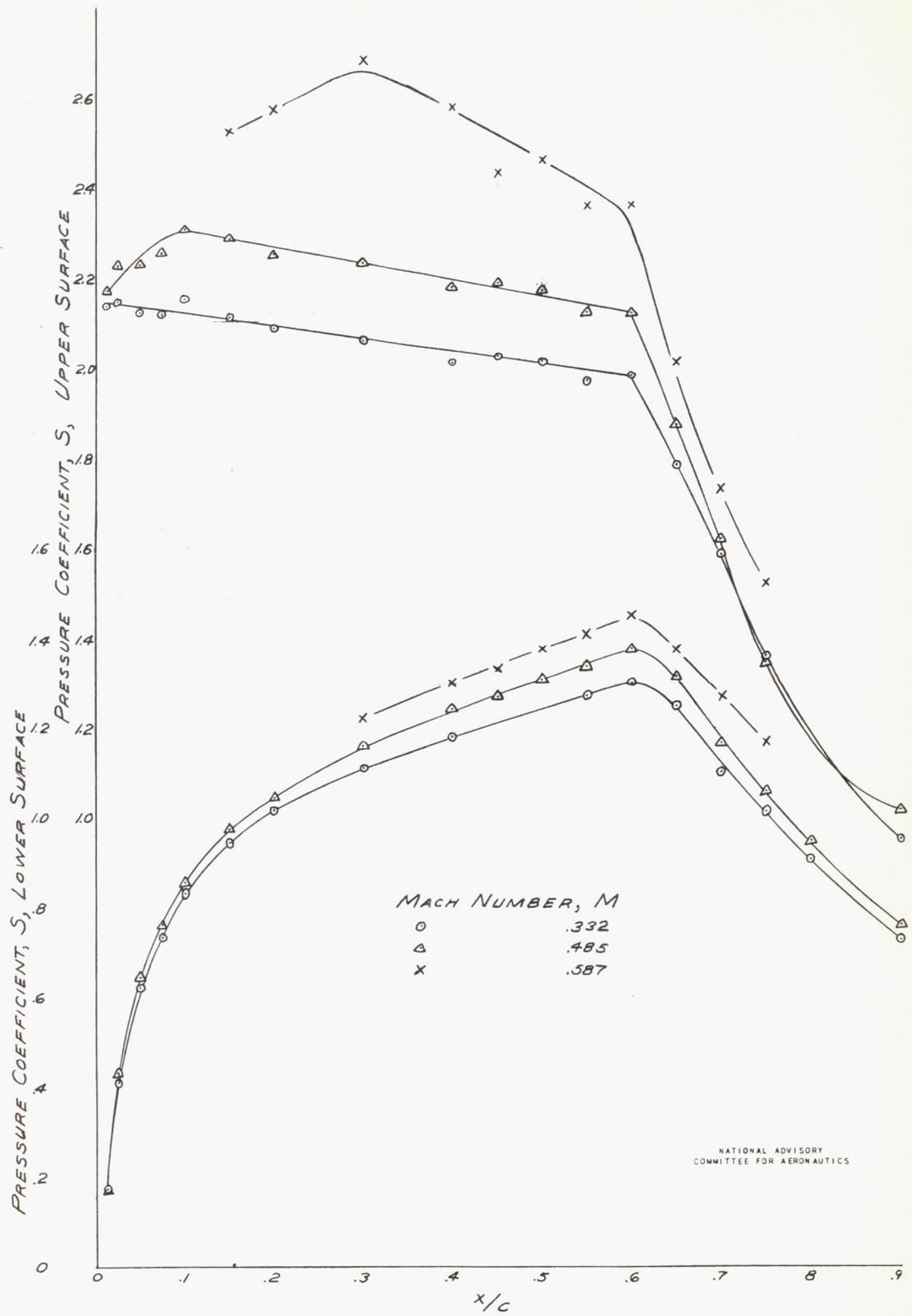
FIGURE 41. — PRESSURE DISTRIBUTION ON THE SMOOTH NACA 66(218)-420
AIRFOIL. α = +4.1°, 5-FOOT CHORD
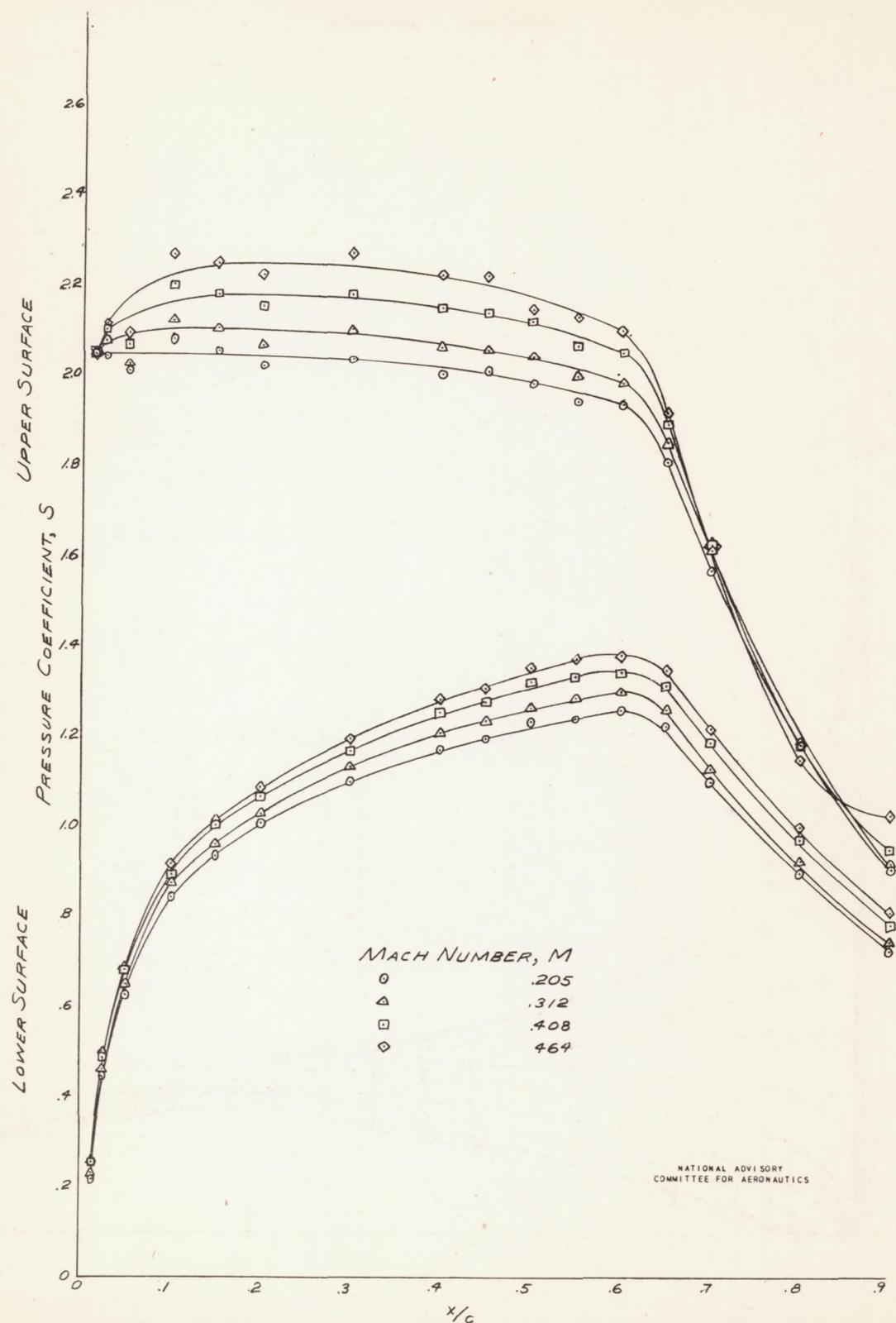
FIGURE 42.- PRESSURE DISTRIBUTION ON THE SMOOTH NACA 66(218)-420
AIRFOIL. $\alpha = +4.3°$, 8-FOOT CHORD.

ANGLE OF ATTACK, ∝

|	
⊙	0°
△	4.1
⊟	8.2
◇	12.3
▲	16.3
◪	20.3
◆	22.3
△	-4.1
◩	-8.2
◩	-12.3
△	-16.4
▷	-20.4
◗	-22.3

PRESSURE COEFFICIENT, S

X/C
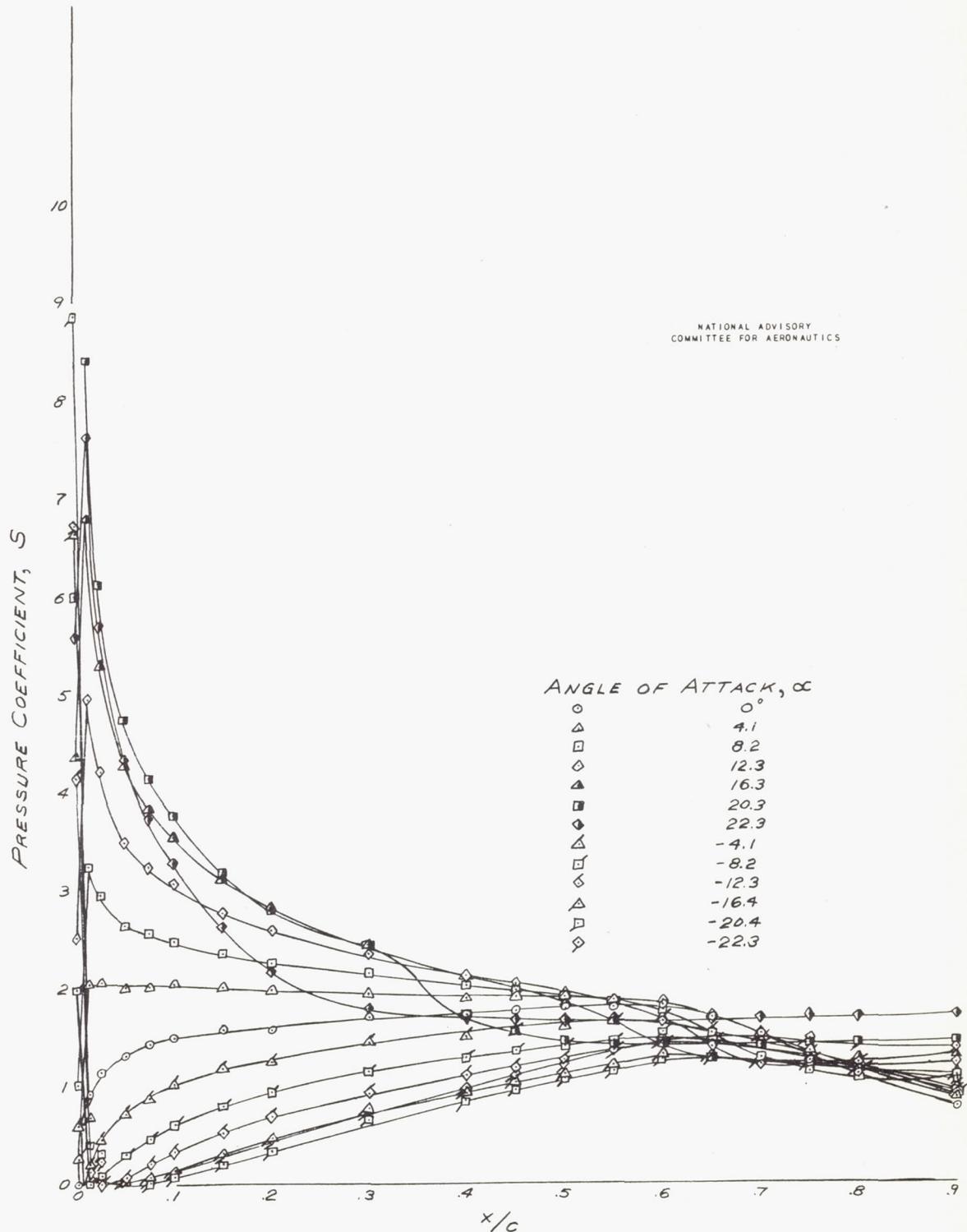
FIGURE 43.— VARIATION OF THE PRESSURE COEFFICIENT ON THE UPPER SURFACE OF THE SMOOTH NACA 66(218)-420 AIRFOIL WITH ANGLE OF ATTACK. 5-FOOT CHORD, M=0.189, R=6.7×10⁶.

...
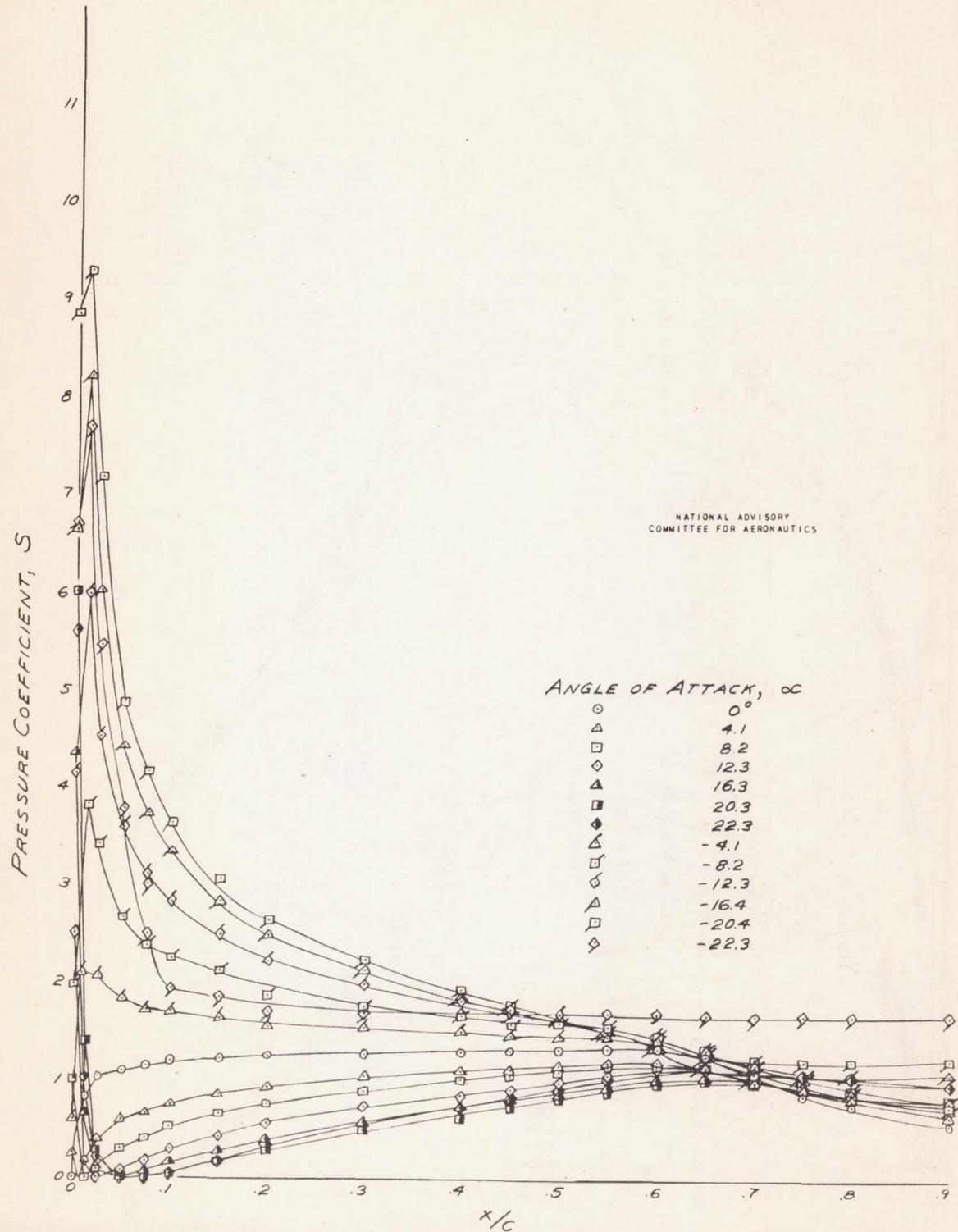
FIGURE 44. – VARIATION OF THE PRESSURE COEFFICIENT ON THE LOWER SURFACE OF THE SMOOTH NACA 66(218)-420 AIRFOIL WITH ANGLE OF ATTACK. 5-FOOT CHORD, M=0.189, R=6.7×10⁶.
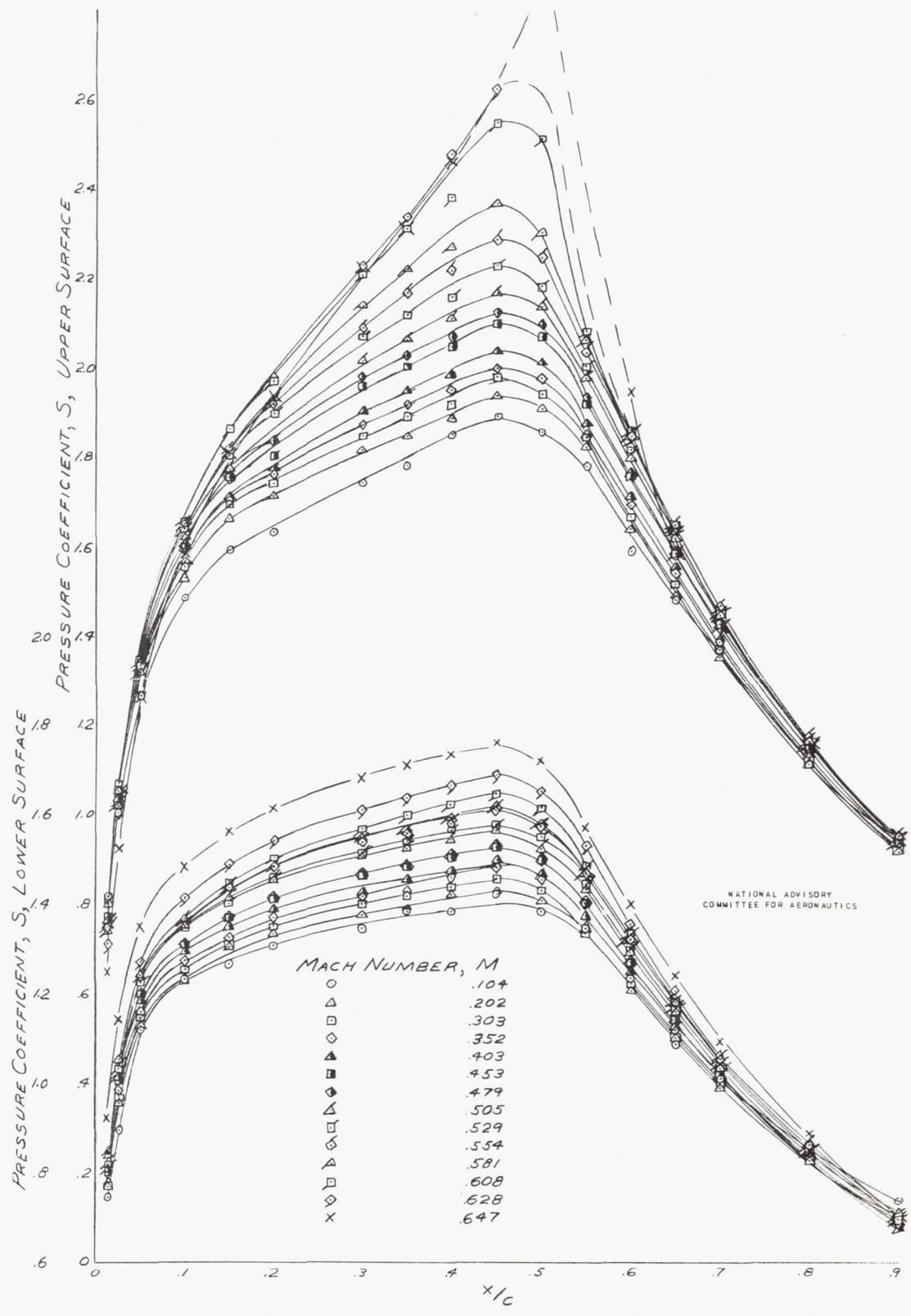
FIGURE 45. - PRESSURE DISTRIBUTION ON THE SMOOTH NACA 65(216)-420
AIRFOIL, ∝ = 0°, 5-FOOT CHORD.
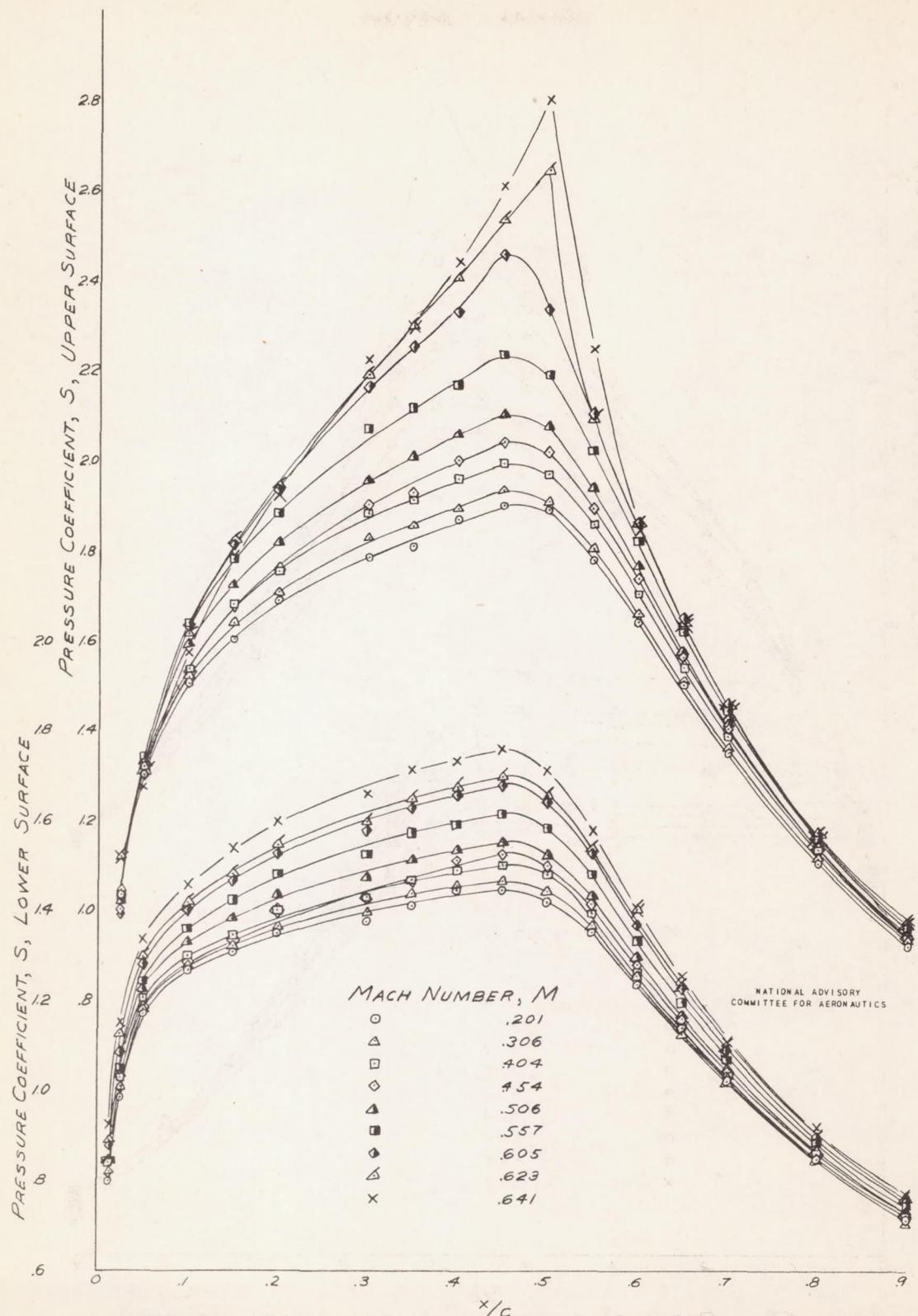
FIGURE 46. — PRESSURE DISTRIBUTION ON THE NACA 65(216)-420 AIRFOIL
WITH ROUGHNESS AT 10-PERCENT CHORD. α = 0°, 5-FOOT CHORD.
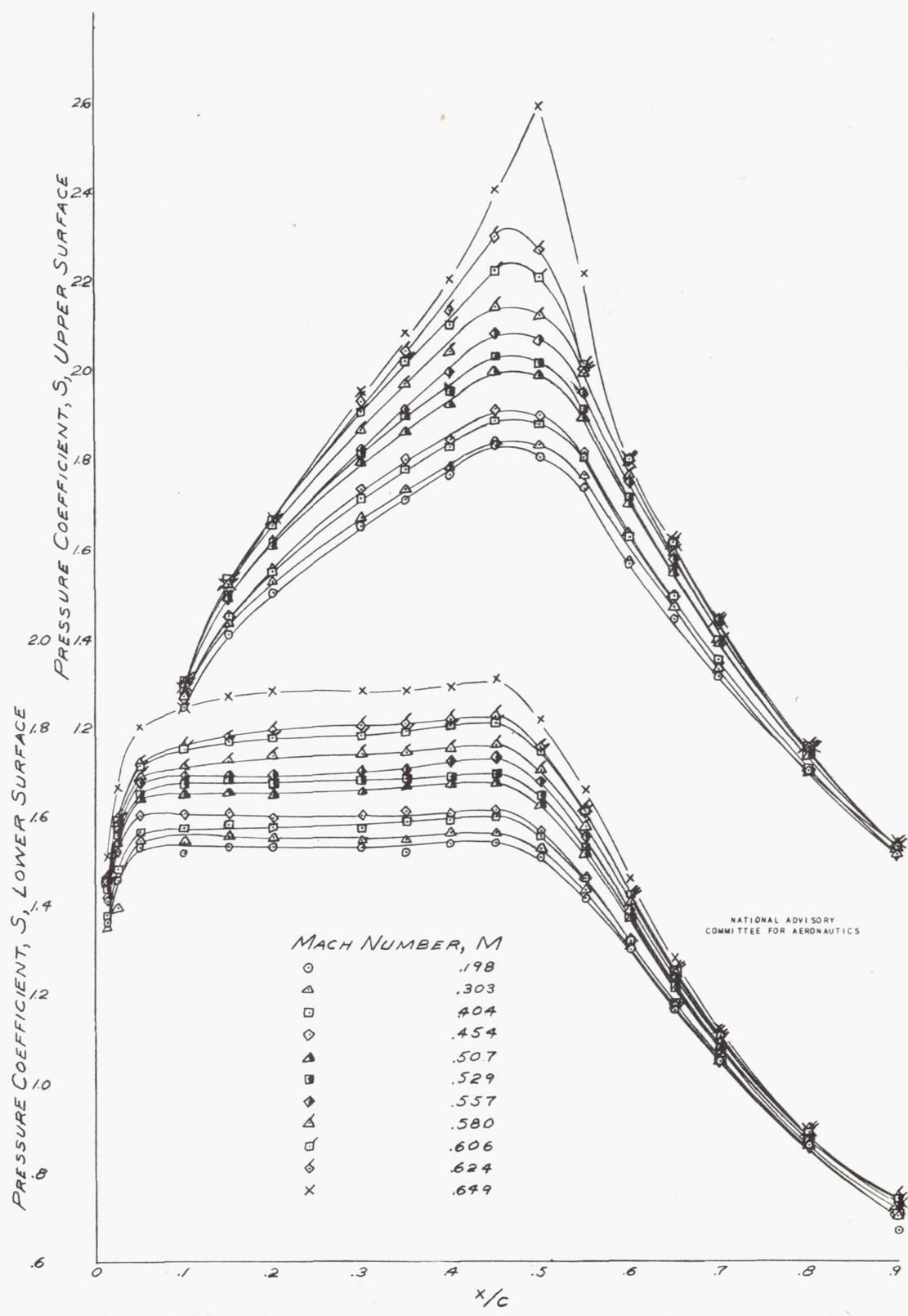
FIGURE 47. – PRESSURE DISTRIBUTION ON THE SMOOTH NACA 65(216)-420
AIRFOIL. ∝ = -2.1°, 5-FOOT CHORD.

PRESSURE COEFFICIENT, S, UPPER SURFACE

PRESSURE COEFFICIENT, S, LOWER SURFACE

2.8
2.6
2.4
2.2
2.0
1.8
1.6
1.4
1.2
1.0
0.8
0.6
0.4
0.2

0   .1   .2   .3   .4   .5   .6   .7   .8   .9

x/c

MACH NUMBER, M

⊙   .089
△   .201
⊡   .303
◇   .404
▲   .503
◨   .557
◆   .577
✕   .603
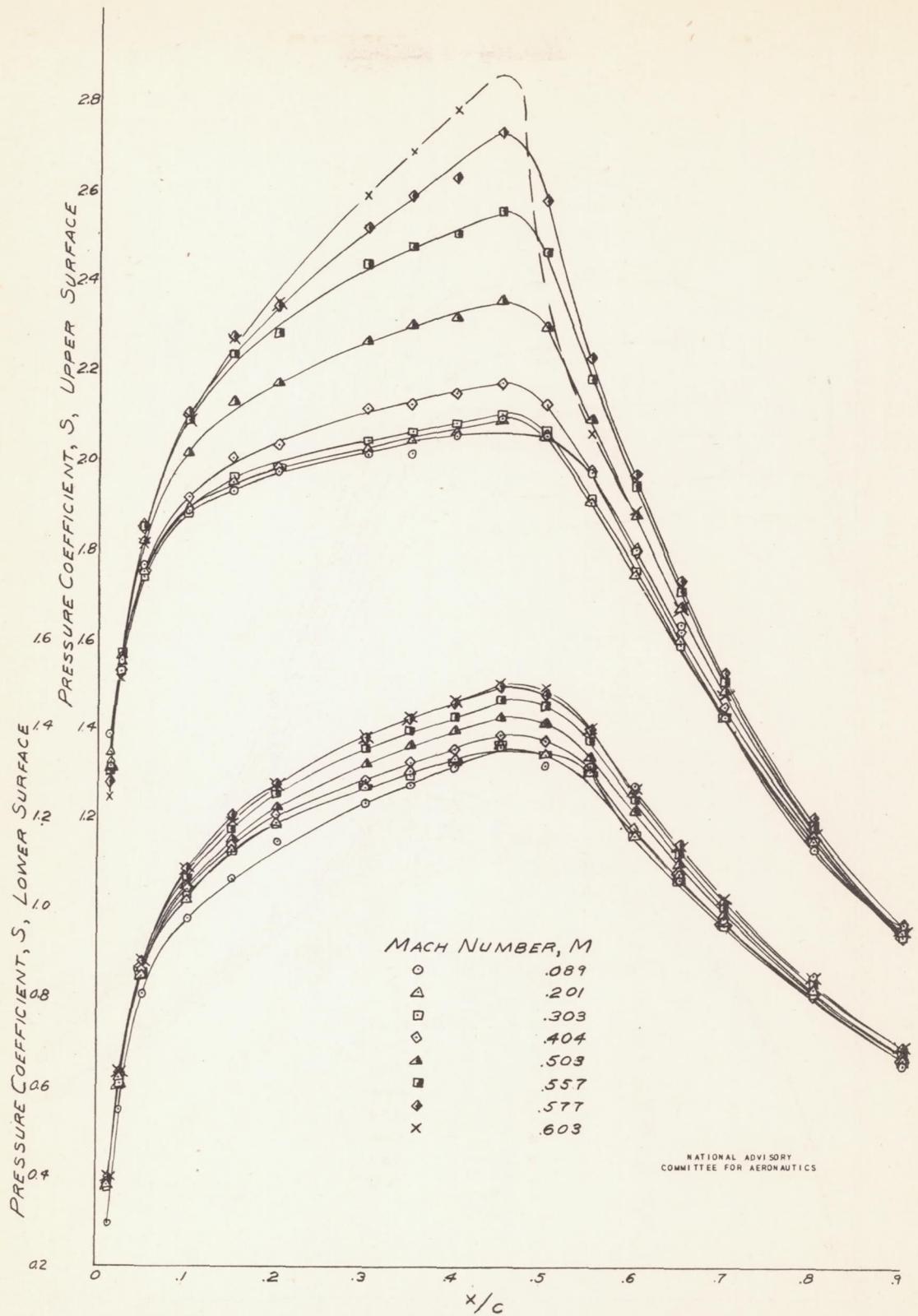
FIGURE 48. - PRESSURE DISTRIBUTION ON THE SMOOTH NACA 65(216)-420
AIRFOIL. $\alpha = +2.1°$; 5-FOOT CHORD.
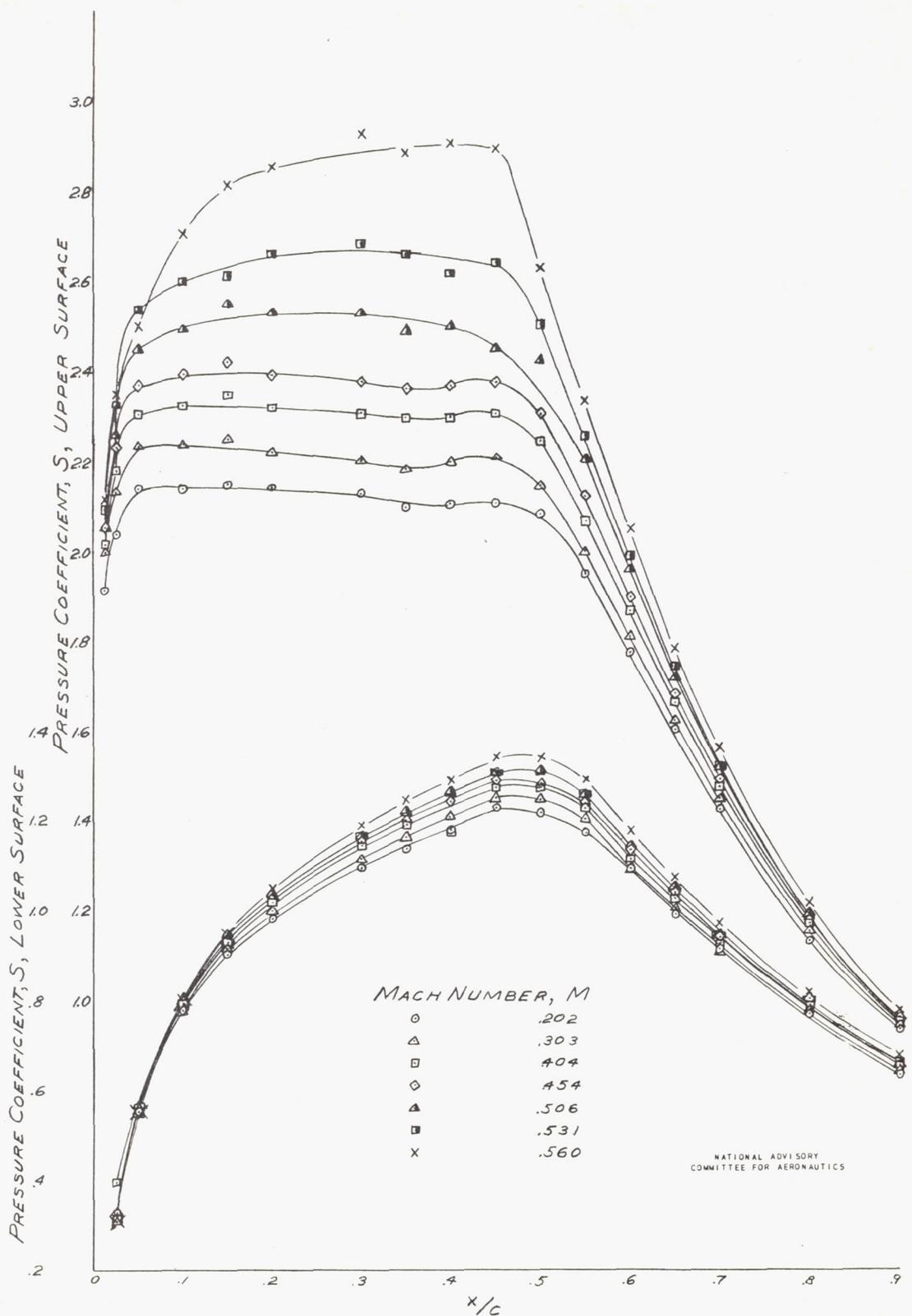
FIGURE 49. — PRESSURE DISTRIBUTION ON THE SMOOTH NACA 6S(216)-420 AIRFOIL. α = + 4.2°, 5-FOOT CHORD.

MACH NUMBER, M

⊙	.202
△	.303
⊡	.404
◇	.454
▲	.506
◼	.531
×	.560

NATIONAL ADVISORY
COMMITTEE FOR AERONAUTICS

ANGLE OF ATTACK, α

⊘	0
△	4.1
⊡	8.2
◇	12.2
▲	16.3
■	20.2
⬦	22.2
△	-4.1
⊡	-8.2
◊	-12.3
△	-16.4
⊡	-20.2

NATIONAL ADVISORY
COMMITTEE FOR AERONAUTICS

PRESSURE COEFFICIENT, S

x/c
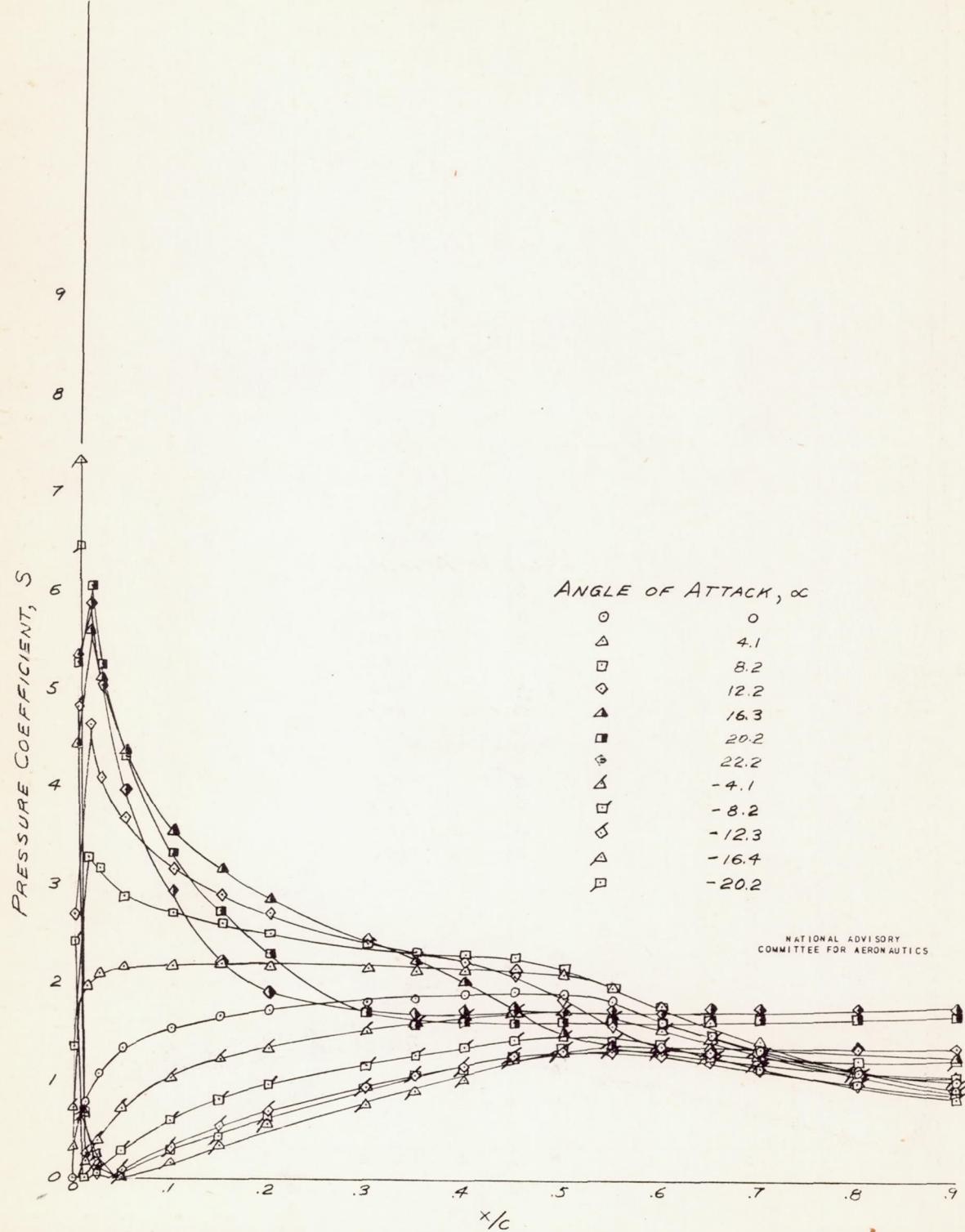
FIGURE 50. - VARIATION OF THE PRESSURE COEFFICIENT ON THE UPPER
SURFACE OF THE SMOOTH NACA 65(216)-420 AIRFOIL WITH
ANGLE OF ATTACK. 5-FOOT CHORD, M=0.197, R=6.8×10^6
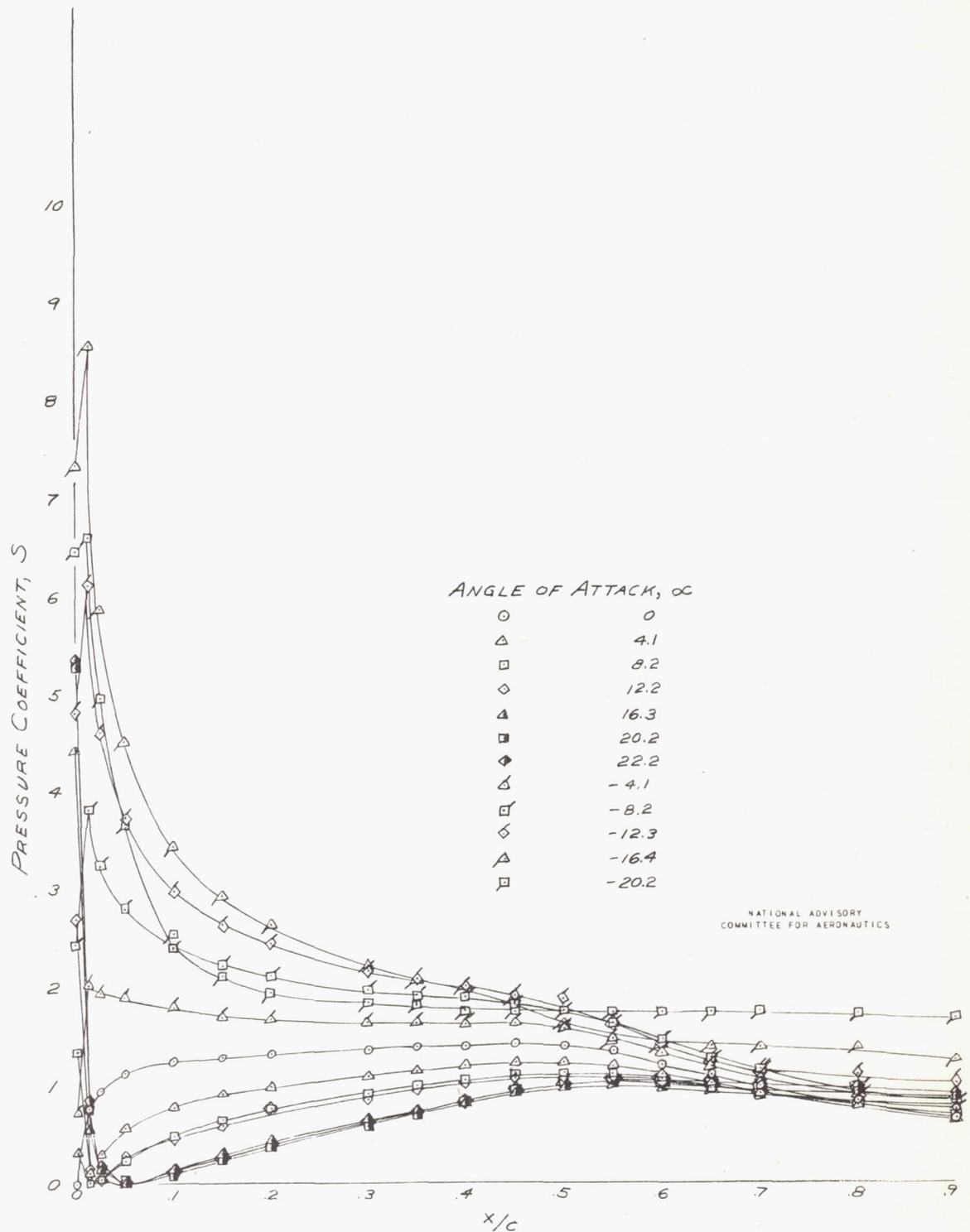
FIGURE 51. - VARIATION OF THE PRESSURE COEFFICIENT ON THE LOWER SURFACE OF THE SMOOTH NACA 65(216)-420 AIRFOIL WITH ANGLE OF ATTACK. 5-FOOT CHORD, M=0.197, R=6.8×10⁶.